

Bayesian Shrinkage Priors for Penalized Synthetic Control Estimators in the Presence of Spillovers

Esteban Fernández-Morales^{1,*}, Arman Oganisian¹, and Youjin Lee¹

¹Department of Biostatistics, Brown University, Providence, RI, United States

* *email*: esteban_fernandez@brown.edu

Abstract

Synthetic control (SC) methods are widely used to evaluate the impact of policy interventions, particularly those targeting specific geographic areas or regions, commonly referred to as units. These methods construct an artificial (*synthetic*) unit from untreated (*control*) units, intended to mirror the characteristics of the treated region had the intervention not occurred. Neighboring areas are often chosen as controls because of their presumed similarity in potential confounders with the treated unit. However, their proximity may cause spillover effects, where the intervention indirectly impacts these controls, resulting in biased estimates. To address this challenge, we propose a Bayesian SC method with distance-based shrinkage priors, designed to estimate causal effects while accounting for spillovers. Modifying traditional penalization techniques, our approach incorporates a weighted distance function that considers both covariate information and spatial proximity to the treated. Rather than simply excluding nearby controls, this framework data-adaptively selects those less likely to be impacted by spillovers, providing a balance between bias and variance reduction. Through simulation studies, we demonstrate the finite-sample properties of our method under varying levels of spillover. We then apply this approach to evaluate the impact of Philadelphia's beverage tax on the sales of sugar-sweetened and artificially sweetened beverages in mass-merchandise stores.

Keywords: Bayesian inference; Beverage tax; Shrinkage priors; Spillover effects; Synthetic control.

1. Introduction

Evaluating the impact of policy interventions is a key area of focus for economists, public health researchers, and policymakers. However, such interventions often produce unintended effects on units not directly targeted. For instance, Philadelphia’s excise tax on sugar-sweetened and artificially sweetened beverages reduced sales within the city but increased sales in neighboring counties (Roberto et al., 2019). Similarly, the legalization of recreational marijuana in Colorado and Washington not only lowered certain crime rates within these states, but also in neighboring states where it remained illegal (Wu et al., 2020).

Despite the potential for spillover effects, many studies evaluating policy impacts have used neighboring units as controls, as they often share similar characteristics (e.g., demographics, socioeconomic factors) with the treated units. However, including controls that may have been indirectly affected by the intervention can bias causal effect estimates. This occurs because such controls no longer accurately represent the hypothetical characteristics of the treated units had the intervention not occurred, resulting in biased estimates. This issue is relevant for two commonly used methods, difference-in-differences (DiD) and synthetic control (SC), whose accuracy depends on the assumption that controls are not affected.

The DiD method estimates the policy effect by comparing changes in outcomes over time between control and treated units (Ashenfelter, 1978; Ashenfelter and Card, 1984). The causal validity of the DiD estimator depends on the parallel trends assumption, which assumes that, in the *absence of the intervention*, the difference in outcomes between the control and treated groups would have remained constant over time. In contrast, the SC method constructs a weighted combination of control units, referred to as the *donor pool*, to estimate the counterfactual outcomes of the treated unit had the intervention not occurred (Abadie et al., 2010; Abadie and Gardeazabal, 2003). The intervention effect is then estimated by comparing the observed outcomes of the treated unit with those of its synthetic counterpart (Abadie and Gardeazabal, 2003).

Although DiD and SC methods are widely used for policy evaluation, their causal interpretations are limited when control units are affected by the intervention (i.e., when spillover effects occur). In the DiD framework, if controls in the comparison group are impacted by spillovers, their outcome trends no longer accurately reflect what would have occurred in the absence of the intervention. Similarly, in the SC method, spillovers affecting the donor pool can worsen the SC’s ability to replicate the treated

unit’s counterfactual outcomes. Consequently, comparing observed and predicted outcomes may result in a biased estimate of the intervention’s true effect.

Recently, several methods have been developed to address spillover effects within the DiD (Butts, 2023; Hettinger et al., 2023; Lee et al., 2023; Verbitsky-Savitz and Raudenbush, 2012) and SC frameworks (Cao and Dowd, 2019; Di Stefano and Mellace, 2024; Grossi et al., 2024; Marinello et al., 2021). Specifically, Grossi et al. (2024) proposed a method for estimating both direct (treatment) and indirect (spillover) effects by using a distance-based criterion to exclude control units from the donor pool. Their approach omits controls directly adjacent to the treated unit, assuming these neighboring units are more likely to be affected by spillovers than those further away. This exclusion criterion is similar to that of Marinello et al. (2021). However, while this method helps mitigate some spillover effects, it may not fully account for units that, though not geographically adjacent, could still be indirectly impacted by the intervention.

Other methods address spillover effects through bias correction techniques. For example, Di Stefano and Mellace (2024) proposed a system of equations to adjust conventional SC estimators for spillover bias. Additionally, Cao and Dowd (2019) introduced a transformation matrix to capture the spillover structure, allowing for the estimation of both direct and indirect effects. However, both approaches require non-singularity conditions, which, if unmet, can prevent the systems of equations from being solvable. Moreover, accurately identifying which units may be affected by spillovers is also crucial to minimize bias in the estimates.

In this work, we propose a novel approach that incorporates Bayesian shrinkage priors to estimate the treatment effect of an intervention in the presence of spillovers. Our method extends traditional penalization techniques, such as the horseshoe and spike-and-slab priors, by incorporating a spatial distance measure between control and treated units – a factor we hypothesize determines the magnitude of spillover effects. This distance-based strategy facilitates a data-driven selection of control units from the donor pool, providing a more flexible alternative to deterministic rule-based criteria. Furthermore, we introduce a weighted distance function that balances the penalization of covariate dissimilarity and spatial proximity to the treated unit. This approach assigns greater weight to controls that closely resemble the treated unit, while reducing potential bias caused by spillover effects.

The remainder of this article is organized as follows. Section 2 introduces the notation and setting, defines the target estimand, and outlines the key causal assumptions. Section 3 details the SC method

within a Bayesian framework, which serves as the basis for our approach, and introduces the proposed distance-based shrinkage priors. Section 4 presents simulation results to assess the finite-sample properties of the proposed method. In Section 5, we demonstrate our approach by evaluating the impact of Philadelphia’s beverage tax on the sales of sugar-sweetened and artificially sweetened beverages. Finally, Section 6 provides concluding remarks and explores potential future research directions.

2. Notations, Assumptions, and Causal Estimands

We consider aggregated units such as cities, states, regions, or other large population areas to which the intervention can be uniquely assigned. Let $i \in [n]$ index the units and $t \in [T]$ index time, where $[m] = \{1, \dots, m\}$ represents the set of integers from 1 to m . The primary outcome for each unit i at time t is denoted by $Y_{it} \in \mathbb{R}$, where we assume a continuous outcome. Our focus is on scenarios where the intervention targets a single treated unit ($i = 1$), implemented at time $T_0 \in \mathbb{N}$, with $T_0 < T$. The remaining $J = n - 1$ units make up the donor pool, serving as potential controls that may be indirectly affected by the intervention. The donor pool outcomes at time t are denoted by $\mathbf{V}_t = (Y_{2t}, \dots, Y_{nt}) \in \mathbb{R}^J$.

Let $Z_{it} \in \{0, 1\}$ denote a time-varying binary treatment indicator, where $Z_{it} = 1$ if unit i is directly targeted by the intervention (i.e., not due to spillovers) at time t . We assume the intervention occurs only once and remains in effect thereafter, implying $Z_{it} \leq Z_{is}$ for $t \leq s$. The treatment status for all n units at time t is represented by the vector $\mathbf{Z}_t = (Z_{1t}, \dots, Z_{nt})$. For each unit i , we observe a q -dimensional vector of pre-intervention (baseline) covariates, $\mathbf{X}_i \in \mathbb{R}^q$. The full set of baseline covariates for all n units is given by $\mathbf{X} = (\mathbf{X}_1, \dots, \mathbf{X}_n)$. We further assume that \mathbf{X}_i includes spatial coordinates, denoted by $\mathbf{P}_i \in \mathbb{R}^k$, where $k \leq q$ represents the number of dimensions in the coordinate system. For example, as elaborated in Section 5, we set $k = 2$, with \mathbf{P}_1 representing the Cartesian coordinates of Philadelphia’s geographic center. For clarity, we denote the history of a variable A up to time t as $\overline{A}_t = (A_1, \dots, A_t)$ and its future trajectory from time t onwards as $\underline{A}_t = (A_t, \dots, A_T)$. In summary, the observed data is given by $\mathbf{O} = (\overline{Y}_{1T_0}, \overline{\mathbf{Z}}_{T_0} = \overline{\mathbf{0}}_n, \overline{\mathbf{V}}_T)$, where $\overline{\mathbf{Z}}_{T_0} = \overline{\mathbf{0}}_n$ indicates that the treatment assignments up to time T_0 are all zero, as the intervention has not yet occurred.

We use the potential outcomes framework (Holland, 1986; Rubin, 1974) to formally define our target estimand and outline the causal assumptions required for its identification. We assume that each unit’s potential outcome at time t depends solely on the intervention status at that time, \mathbf{Z}_t , rather than the

entire intervention history, $(\mathbf{Z}_1, \dots, \mathbf{Z}_T)$. In settings with spillovers, the Stable Unit Treatment Value Assumption (SUTVA) (Rubin, 1974) is violated because the treatment status of one unit can influence the potential outcomes of others.

Consequently, the potential outcome for unit i at time t is defined as $Y_{it}(\mathbf{z}_t)$, where $\mathbf{z}_t \in \{0, 1\}^n$ denotes the treatment status vector for the entire population at time t . For example, $Y_{it}(\mathbf{0}_n)$ represents the potential outcome under no intervention, with $\mathbf{0}_n = (0, \dots, 0)$ being a zero vector of length n . Similarly, $Y_{it}(\mathbf{z}_t^*)$ denotes the potential outcome under the observed intervention, where $\mathbf{z}_t^* = (1, \mathbf{0}_J)$ indicates that only a single unit ($i = 1$) is treated. For instance, in Section 5, this corresponds to Philadelphia being the only treated unit (county) under the intervention (beverage tax). We define the target estimand as the causal effect of the intervention on the treated unit for $t > T_0$:

$$\tau_t := Y_{1t}(\mathbf{z}_t^*) - Y_{1t}(\mathbf{0}_n). \quad (1)$$

In our context, $Y_{1t}(\mathbf{0}_n)$ represents the unobserved potential outcome, as the intervention was indeed implemented, while $Y_{1t}(\mathbf{z}_t^*)$ is observable for all periods following the intervention. To identify τ_t from the observed data \mathbf{O} , we impose the following assumptions:

Assumption 1 (No anticipation). The intervention has no effect on outcomes before its implementation (Abadie et al., 2010), implying that $Y_{1t} = Y_{1t}(\mathbf{0}_n)$ for all $t \in [T_0]$.

Assumption 2 (Consistency). There are no hidden versions of the treatment (Rubin, 1980), directly linking observed and potential outcomes, i.e., if $\mathbf{Z}_t = \mathbf{z}_t$, then $Y_{it} = Y_{it}(\mathbf{z}_t)$ for all $t \in [T]$, $\mathbf{z}_t \in \{0, 1\}^n$.

Assumption 3 (Covariate independence and sequential ignorability). Given the observed history, the current and future potential outcomes are independent of the baseline covariates \mathbf{X} and current treatment assignments \mathbf{Z}_t , i.e., $\underline{Y}_{1t}(\mathbf{z}_t) \perp (\mathbf{X}, \mathbf{Z}_t) \mid \bar{\mathbf{V}}_t, \bar{Y}_{1(t-1)}, \bar{\mathbf{Z}}_{t-1}$ for all $t \in [T]$, $\mathbf{z}_t \in \{0, 1\}^n$.

Assumptions 1-3 are essential for connecting the unobservable quantities with observable data. Unlike standard ignorability assumptions, Assumption 3 ensures that \mathbf{O} captures all confounding factors by conditioning not only on the treated unit's past outcomes, $\bar{Y}_{1(t-1)}$, but also on variables from other units, $\bar{\mathbf{V}}_t$ and $\bar{\mathbf{Z}}_{t-1}$. Conditioning on these variables is sufficient to account for confounding, eliminating the need to explicitly condition on \mathbf{X}_1 (or \mathbf{X}), as they implicitly capture the effects of the covariates. In Section 3, we introduce prior distributions that incorporate \mathbf{X} , indirectly capturing the relationship

between covariates and outcomes.

Under Assumptions 1-3, we can estimate τ_t by imputing the unobservable (missing) potential outcomes, $\mathbf{Y}^m = \{Y_{1t}(\mathbf{O}_n) : t > T_0\}$, within a Bayesian causal framework (Li et al., 2023; Oganisian and Roy, 2021). We denote the parameters governing the outcome distribution by $\boldsymbol{\theta} \in \Theta$, where Θ is the parameter space. It is assumed that $\boldsymbol{\theta}$ remains constant across all periods, implying that the relative influence of other units' outcomes and the treated unit's past outcomes on its current outcome does not change over time. The imputation process depends on the posterior predictive distribution (PPD) for \mathbf{Y}^m given \mathbf{O} and \mathbf{X} :

$$p(\mathbf{Y}^m \mid \mathbf{O}, \mathbf{X}) \propto \int_{\Theta} \prod_{t>T_0} p(Y_{1t} \mid \bar{\mathbf{Z}}_t = \bar{\mathbf{O}}_n, \bar{\mathbf{V}}_t, \bar{Y}_{1(t-1)}, \boldsymbol{\theta}) \pi(\boldsymbol{\theta} \mid \mathbf{O}, \mathbf{X}) d\boldsymbol{\theta}. \quad (2)$$

This expression marginalizes the distribution of the missing post-intervention outcome Y_{1t} , conditioned on the observed history and $\boldsymbol{\theta}$, over the posterior distribution (PD) of $\boldsymbol{\theta}$ given \mathbf{O} and \mathbf{X} . Imputed values for \mathbf{Y}^m can be drawn from the PPD using Monte Carlo methods, as detailed in Section 3.

The process involves specifying a model, $p(Y_{1t} \mid \bar{\mathbf{Z}}_t = \bar{\mathbf{O}}_n, \bar{\mathbf{V}}_t, \bar{Y}_{1(t-1)}, \boldsymbol{\theta})$, for the observed outcomes of the treated unit. This serves as the foundation for imputing future post-intervention outcomes and for deriving the PD of $\boldsymbol{\theta}$, denoted by $\pi(\boldsymbol{\theta} \mid \mathbf{O}, \mathbf{X})$. In Section 3, we propose an SC-based model that incorporates a selection procedure for control units, aimed at minimizing bias from spillover effects. A detailed derivation of the PPD is provided in the Supporting Information.

3. Methods

Models in the Bayesian SC literature typically express the treated unit's potential outcomes, in the absence of intervention, as a function of the donor pool outcomes (Brodersen et al., 2015; Kim et al., 2020; Pang et al., 2022). Following this approach, we propose the following model specification for $t \in [T_0]$:

$$Y_{1t} \mid \bar{\mathbf{Z}}_t = \bar{\mathbf{O}}_n, \bar{\mathbf{V}}_t, \bar{Y}_{1(t-1)}, \boldsymbol{\theta} \sim \text{Normal}(m(\bar{\mathbf{V}}_t, \bar{Y}_{1(t-1)}), \phi), \quad (3)$$

$$m(\bar{\mathbf{V}}_t, \bar{Y}_{1(t-1)}) = \mathbf{V}'_t \boldsymbol{\beta} + \varphi Y_{1(t-1)},$$

where $\boldsymbol{\theta} = (\boldsymbol{\beta}, \varphi, \phi)$, with $\boldsymbol{\beta} \in \mathbb{R}^J$, $\varphi \in \mathbb{R}$, and $\phi \in \mathbb{R}^+$, represents the model parameters. In this framework, the outcomes are assumed to follow a normal distribution, with a mean function $m(\cdot)$ that depends on the observed history.

We adopt a Markov assumption to simplify the history dependence, restricting it to the current donor pool outcomes, \mathbf{V}_t , and the previous outcome for the treated unit, $Y_{1(t-1)}$. The parameter φ captures the longitudinal dependence on the prior outcome $Y_{1(t-1)}$, while ϕ is the scale parameter governing the variance of the outcomes, both assumed to be constant over time. The SC coefficients, $\boldsymbol{\beta} = (\beta_2, \dots, \beta_n)$, function similarly to traditional SC weights by generating a weighted combination, $\mathbf{V}'_t\boldsymbol{\beta}$, of the donor pool at time t . This term helps predicts the treated unit's expected outcome in the absence of the intervention, $\mathbb{E}[Y_{1t}(\mathbf{O}_n) \mid \bar{\mathbf{V}}_t, \bar{Y}_{1(t-1)}, \boldsymbol{\theta}] \equiv m(\bar{\mathbf{V}}_t, \bar{Y}_{1(t-1)})$. For the prior specification of $\boldsymbol{\theta}$, we assign standard priors to the parameters φ and ϕ . The prior for φ is $\text{Normal}(\mu_\varphi, \sigma_\varphi^2)$, with $\mu_\varphi \in \mathbb{R}$ and $\sigma_\varphi \in \mathbb{R}^+$. We use a half-Student's t prior for ϕ , denoted by $\text{Half-Student}(\nu_\phi, 0, \tau_\phi^2)$, where $\nu_\phi, \tau_\phi \in \mathbb{R}^+$.

In this work, we focus on specifying the prior for $\boldsymbol{\beta}$. Let $\boldsymbol{\gamma} \in \Gamma$ represent a set of hyperparameters that partially or fully govern the distribution of $\boldsymbol{\beta}$, where Γ denotes the corresponding parameter space. It is important to note that $\boldsymbol{\theta}$ and $\boldsymbol{\gamma}$ are distinct parameter sets: $\boldsymbol{\theta}$ governs the distribution of Y_{1t} , while $\boldsymbol{\gamma}$ governs the distribution of $\boldsymbol{\beta}$. The prior distribution of $\boldsymbol{\beta}$ conditional on ϕ and $\boldsymbol{\gamma}$ is denoted by $\pi(\boldsymbol{\beta} \mid \phi, \boldsymbol{\gamma})$. Additionally, we specify a data-dependent hyperprior on $\boldsymbol{\gamma}$ conditional on the covariates \mathbf{X} , expressed as $\pi(\boldsymbol{\gamma} \mid \mathbf{X})$. Given these model and prior specifications, the PD of $\boldsymbol{\theta}$ is given by:

$$\begin{aligned} \pi(\boldsymbol{\theta} \mid \mathbf{O}, \mathbf{X}) &\propto \prod_{t \leq T_0} p(Y_{1t} \mid \bar{\mathbf{Z}}_t = \bar{\mathbf{0}}_n, \bar{\mathbf{V}}_t, \bar{Y}_{1(t-1)}, \boldsymbol{\theta}) \pi(\varphi) \pi(\phi) \pi(\boldsymbol{\beta} \mid \mathbf{X}, \phi), \\ \pi(\boldsymbol{\beta} \mid \mathbf{X}, \phi) &= \int_{\Gamma} \pi(\boldsymbol{\beta} \mid \phi, \boldsymbol{\gamma}) \pi(\boldsymbol{\gamma} \mid \mathbf{X}) d\boldsymbol{\gamma}, \end{aligned} \tag{4}$$

where $\pi(\boldsymbol{\beta} \mid \mathbf{X}, \phi)$ is obtained by marginalizing the prior distribution of $\boldsymbol{\beta}$ over the data-dependent hyperprior distribution of $\boldsymbol{\gamma}$. The specific densities (normal, half-Student's t) can then be incorporated to perform posterior sampling of $\boldsymbol{\theta}$. A detailed derivation of the PD is provided in the Supporting Information.

We introduce two distance-based shrinkage priors for $\boldsymbol{\beta}$ and $\boldsymbol{\gamma}$, based on conventional penalization techniques: the *distance horseshoe* (DHS) and *distance spike-and-slab* (DS2). These priors incorporate spatial distance relative to the treated unit to adjust the degree of shrinkage applied to the SC coefficients, where geographically closer controls exhibit higher shrinkage. While spatial proximity is often associated with a higher likelihood of spillovers, relying strictly on this information to determine shrinkage can lead to bias or statistical inefficiencies. This problem occurs when geographically close controls are in reality unaffected by spillovers, but still share significant similarities with the treated unit. Therefore, balancing spatial distance with additional factors is crucial for improving model performance.

3.1 Weighted Distance Function

Although spatial locations are included as part of the covariates, their role differs from that of the other variables in \mathbf{X}_i . Selecting controls based on spatial proximity to the treated unit may increase bias due to spillovers, whereas similarities in other covariates (potential confounders) generally help reduce confounding bias. To account for these distinct roles, we define \mathbf{X}_i^{-p} as the set of covariates excluding \mathbf{P}_i .

We propose a *weighted distance* that integrates both covariate similarities and spatial distance to the treated unit, which is then used to determine the degree of shrinkage. This distance is defined as a convex combination of covariate dissimilarity, d_X , and spatial proximity, d_P , between control unit $i \in [n] \setminus \{1\}$ and the treated unit ($i = 1$). Each component is specified as follows:

$$d_X(\mathbf{X}_i^{-p}, \mathbf{X}_1^{-p}) = 1/(1 + \|\mathbf{X}_i^{-p} - \mathbf{X}_1^{-p}\|) \quad \text{and} \quad d_P(\mathbf{P}_i, \mathbf{P}_1) = \|\mathbf{P}_i - \mathbf{P}_1\|/S,$$

where $\|\cdot\|$ denotes the Euclidean norm, and $S \in \mathbb{R}^+$ is a scaling factor representing the maximum possible distance between units. Both d_X and d_P are normalized to lie within the unit interval $[0, 1]$. Furthermore, we use the Euclidean norm because of its general applicability. The covariates should be standardized, with spatial locations defined by the units' centroids, making the Euclidean norm an appropriate choice for measuring both covariate dissimilarity and spatial distance. Alternative measures for d_X include the Jaccard index (Jaccard, 1912) for binary or categorical covariates, or the Mahalanobis distance (Mahalanobis, 1936) to account for correlations among covariates.

Given d_X and d_P , the weighted distance between control unit i and the treated unit is defined as

$$d_C(\mathbf{X}_i, \mathbf{X}_1) = \kappa_d \cdot d_X(\mathbf{X}_i^{-p}, \mathbf{X}_1^{-p}) + (1 - \kappa_d) \cdot d_P(\mathbf{P}_i, \mathbf{P}_1), \quad (5)$$

where $\kappa_d \in [0, 1]$ serves as the *importance weight*, determining the relative emphasis on covariate dissimilarity versus spatial proximity. In this framework, when $\kappa_d = 1$, the penalization is based solely on covariate dissimilarities for constructing the SC; when $\kappa_d = 0$, the priority is entirely on spatial distance to mitigate spillover effects in control selection. For values between zero and one, both factors are considered, with a greater dependence on covariates as κ_d increases.

3.2 Defining the Distance-based Priors

To incorporate the weighted distance $d_{i,1}^C := d_C(\mathbf{X}_i, \mathbf{X}_1)$ given κ_d into the priors, we first propose an adaptation of the horseshoe prior (Carvalho et al., 2010). This prior is well-known for handling sparsity, providing a natural mechanism for variable selection, and accommodating large sample sizes. Therefore, it can be useful when the number of control units significantly exceeds the number of pre-intervention outcomes (i.e., $T_0 \ll J$). We assume that each individual SC coefficient β_i in (3) follows a separate normal prior with corresponding hyperpriors, specified for $i \in [n] \setminus \{1\}$:

$$\begin{aligned}\beta_i &| \phi, \lambda_i, \zeta \sim \text{Normal}(0, \phi \lambda_i^2 \zeta^2), \\ \lambda_i &| \mathbf{X}_i, \mathbf{X}_1 \sim \text{Cauchy}^+(0, d_{i,1}^C), \\ \zeta &\sim \text{Cauchy}^+(0, 1),\end{aligned}\tag{6}$$

where $\zeta \in \mathbb{R}^+$ is the global shrinkage parameter shared by all donors, $\lambda_i \in \mathbb{R}^+$ is the local shrinkage parameter, and $\phi \in \mathbb{R}^+$ is the variance term for the outcomes in (3). The set of hyperparameters is denoted by $\gamma = (\lambda_2, \dots, \lambda_n, \zeta)$, where only λ_i depends on the baseline covariates \mathbf{X}_i and \mathbf{X}_1 . The global parameter ζ controls the overall shrinkage of the coefficients β_i toward zero, while the local parameters λ_i allow individual coefficients to deviate from this shrinkage (Piironen and Vehtari, 2017). By incorporating the weighted distance $d_{i,1}^C$ into the variance of the local parameter λ_i , we introduce a distance-dependent adjustment: a smaller weighted distance results in greater shrinkage of the corresponding coefficient β_i toward zero. We refer to this prior specification as the DHS.

Alternatively, we propose the DS2 prior, which extends its traditional counterpart (George and McCulloch, 1993; Mitchell and Beauchamp, 1988) by incorporating $d_{i,1}^C$. We assume that each individual coefficient β_i follows a separate two-component mixture distribution, defined as follows for $i \in [n] \setminus \{1\}$:

$$\begin{aligned}\beta_i &| \phi, \omega_i, \nu \sim (1 - \omega_i)\delta_0 + \omega_i \text{Normal}(0, \phi \nu^2), \\ \omega_i &:= \mathbb{1}(d_{i,1}^C > \rho), \\ \nu &\sim \text{Cauchy}^+(0, 1),\end{aligned}\tag{7}$$

where $\omega_i \in \{0, 1\}$ indicates the component assignment, $\nu^2 \in \mathbb{R}^+$ is the variance parameter for the normally distributed component, and $\phi \in \mathbb{R}^+$ is the variance term for the outcomes. Similarly, the set of

hyperparameters is denoted by $\boldsymbol{\gamma} = (\omega_2, \dots, \omega_n, \nu)$, where each ω_i depends on the covariates \mathbf{X}_i and \mathbf{X}_1 . The *spike* component, represented by the Dirac delta function $\delta_0(u)$, sharply shrinks certain coefficients by concentrating its probability mass at zero. The *slab* component, defined by the normal distribution, ensures that the remaining coefficients β_i , which are not shrunk toward zero, are modeled regularly without any shrinkage.

In our framework, the spike component significantly reduces the influence of certain units in the SC, while the slab component allows others to make substantial contributions. To implement this, we set the parameter ω_i using a distance-dependent assignment mechanism with a user-specified cutoff $\rho \in [0, 1]$. From an interpretative perspective, when the importance weight κ_d is zero (i.e., $\kappa_d = 0$), the cutoff ρ denotes the maximum spatial distance within which control units are excluded from the donor pool. This deterministic approach uses an indicator function, $\mathbb{1}(\cdot)$, to assign each coefficient to either the spike or slab component based on $d_{i,1}^C$. Lastly, we provide a table of key notations and Bayesian graphical models for each prior in the Supporting Information, with particular emphasis on the hyperparameters $\boldsymbol{\gamma}$, which vary based on the selected prior.

3.3 Posterior Sampling Algorithm

Under the model and prior specifications in the previous sections, we can generate draws of $\boldsymbol{\theta}$ by sampling from its PD. Since this distribution lacks a closed-form solution, posterior sampling of $\boldsymbol{\theta}$ can be carried out by Markov chain Monte Carlo (MCMC) techniques, such as the Metropolis-Hastings algorithm (Hastings, 1970) or Metropolis-Hastings-within-Gibbs sampling (Robert, 2015). After obtaining a set of M draws, denoted by $\boldsymbol{\theta}^{(r)} = (\boldsymbol{\beta}^{(r)}, \varphi^{(r)}, \phi^{(r)})$, the missing potential outcomes \mathbf{Y}^m can be imputed using the following sequential sampling approach, for $t > T_0$ and $r \in [M]$:

$$Y_{1t}^{(r)}(\mathbf{0}_n) \mid \bar{\mathbf{Z}}_t = \bar{\mathbf{0}}_n, \bar{\mathbf{V}}_t, \bar{Y}_{1(t-1)}^{(r)}, \boldsymbol{\theta}^{(r)} \sim \text{Normal}(m(\bar{\mathbf{V}}_t, \bar{Y}_{1(t-1)}^{(r)}), \phi^{(r)}),$$

$$m(\bar{\mathbf{V}}_t, \bar{Y}_{1(t-1)}^{(r)}) = \mathbf{V}'_t \boldsymbol{\beta}^{(r)} + \varphi^{(r)} Y_{1(t-1)}^{(r)}.$$

This procedure is based on the PPD in (2), where its causal validity holds under Assumptions 1-3. Subsequently, a posterior estimate of the intervention effect can be computed by $\tau_t^{(r)} = Y_{1t} - Y_{1t}^{(r)}(\mathbf{0}_n)$. Using the MCMC samples, summary statistics such as credible intervals, posterior means, and posterior probabilities can be obtained.

4. Simulation Study

Through a series of numerical experiments, we assess the finite-sample performance of our proposed priors, as defined in (6) and (7). These experiments explore a range of scenarios with varying magnitudes of spillover effects, from none to cases where up to half of the donor pool is affected. In each scenario, we consider $T_0 = 30$ pre-intervention periods and $J = 50$ control units, aligning with the data structure outlined in Section 5. We then estimate the treatment effect τ_t in (1) for a single post-intervention period, specifically at $t = T_0 + 1$.

We consider two baseline covariates, $\mathbf{X}_i \stackrel{iid}{\sim} \text{MVN}(\mathbf{0}_2, \mathbf{I}_2)$, and simulate the spatial distance from each control unit to the treated unit using a truncated normal distribution, $d_i^P := d_P(\mathbf{P}_i, \mathbf{P}_1) \stackrel{iid}{\sim} \text{Normal}_{[0, \infty)}(0, 1)$ for $i \in [n] \setminus \{1\}$, with the distance from the treated unit to itself set to $d_1^P \equiv 0$. Next, we generate the observed outcomes and the potential outcomes in the absence of the intervention using a linear three-factor model as described in Cao and Dowd (2019), for $i \in [n]$ and $t \in [T]$:

$$\begin{aligned}
 Y_{it} &= Y_{it}(\mathbf{0}_n) + \tau_t Z_{it} + \xi_t(1 - Z_{it})\mathbb{1}(t > T_0) \exp(-d_i^P) \mathbb{1}(d_i^P < \rho^*), \\
 Y_{it}(\mathbf{0}_n) &= \delta_t + \boldsymbol{\vartheta}^T \mathbf{X}_i + \mathbf{f}_t^T \boldsymbol{\mu}_i + \epsilon_{it}, \\
 \epsilon_{it} &\stackrel{iid}{\sim} \text{Normal}(0, 1).
 \end{aligned}$$

Here, $\delta_t \in \mathbb{R}$ represents a common factor across units, $\boldsymbol{\vartheta} = (\vartheta_1, \vartheta_2) \in \mathbb{R}^2$ is a vector of baseline covariate effects, $\mathbf{f}_t = (f_{1t}, f_{2t}, f_{3t}) \in \mathbb{R}^3$ is a vector of time-varying common factors, $\boldsymbol{\mu}_i = (\mu_{i1}, \mu_{i2}, \mu_{i3}) \in \mathbb{R}^3$ is a vector of factor loadings, and $\epsilon_{it} \in \mathbb{R}$ is an unobserved transitory shock. We set the intervention effect to $\tau_t = 7$ and the spillover effect to $\xi_t = -10$. The cutoff $\rho^* \in \mathbb{R}^+$ determines the proportion of control units affected by spillover. In this setup, the spillover effect is constrained to a specific range, with its magnitude depending on the distance from the treated unit.

We apply the weighted distance function to both the DHS and DS2 priors, using varying values of $\kappa_d \in \{0.0, 0.1, 0.5, 1.0\}$ in (5), where the weighted distance $d_{i,1}^C$ is computed for each control unit i based on d_i^P and \mathbf{X}_i . The cutoff ρ in (7) is set to exclude approximately 25% of the units in the donor pool, focusing on either the spatially nearest or most dissimilar units relative to the treated unit, depending on the selected κ_d value. For comparison, we also consider two alternative approaches for estimating the treatment effect using the same donor pool. The first alternative is the Bayesian structural

time-series (BSTS) model, which utilizes a state-space framework to predict counterfactual outcomes, accounting for trends, seasonality, and other sources of variation in time-series data (Brodersen et al., 2015). The second alternative is the generalized synthetic control (GSC) method, which integrates the SC methodology with a linear fixed-effects model to impute counterfactual outcomes, using a parametric bootstrap for uncertainty estimation (Xu, 2017). While these comparison methods allow for additional components in the outcome model, better aligning with the data-generating process, they do not utilize spatial information from controls units to account for spillovers. As a result, while bias from model misspecification bias is less likely, there may be significant bias due to spillovers.

To evaluate the performance of the DHS and DS2 priors, we conduct simulations across 1,000 independent replications and report their empirical results, including relative bias and coverage probability of the 95% credible (or confidence) intervals. Our priors are implemented using Stan (Carpenter et al., 2017), which uses a Hamiltonian Monte Carlo algorithm to generate posterior draws. For each replication, we run a single MCMC chain with 10,000 iterations, discarding the first half as burn-in. The hyperparameters for the prior distributions of φ and ϕ are set as $\mu_\varphi = 0$, $\sigma_\varphi = 3$, $\nu_\phi = 4$, and $\tau_\phi = 1$. The BSTS model is implemented using the `CausalImpact` R package, with a single MCMC chain of 10,000 iterations, discarding the first half as burn-in and applying default model settings (Brodersen et al., 2015). Similarly, the GSC method is implemented using the `gsynth` R package, using cross-validation to select the optimal number of factors, two-way fixed effects, and 1,000 bootstrap replicates for estimating confidence intervals (Xu, 2017).

Figure 1 shows the relative bias and the coverage probability of the 95% credible (or confidence) intervals for our proposed priors, compared with the alternative methods, across different values of κ_d and varying percentages of the donor pool affected by spillover. Across all κ_d values, both bias and deviation from nominal coverage increase as the percentage of affected control units rises. However, the DHS and DS2 priors show smaller changes, suggesting they are more robust in terms of bias and coverage probability. At lower κ_d values ($\kappa_d = 0.0, 0.1$), both priors exhibit nearly nominal coverage up to 30% spillover. However, as spillover exceeds 40%, undercoverage becomes more evident for both priors. The deviation from nominal coverage is even greater when κ_d increases to 0.5 or 1.0, as both priors consider little to no spatial information from control units. Both comparison methods (BSTS and GSC) show greater bias than the priors at all percentages, particularly at lower κ_d values ($\kappa_d = 0.0, 0.1$). The BSTS

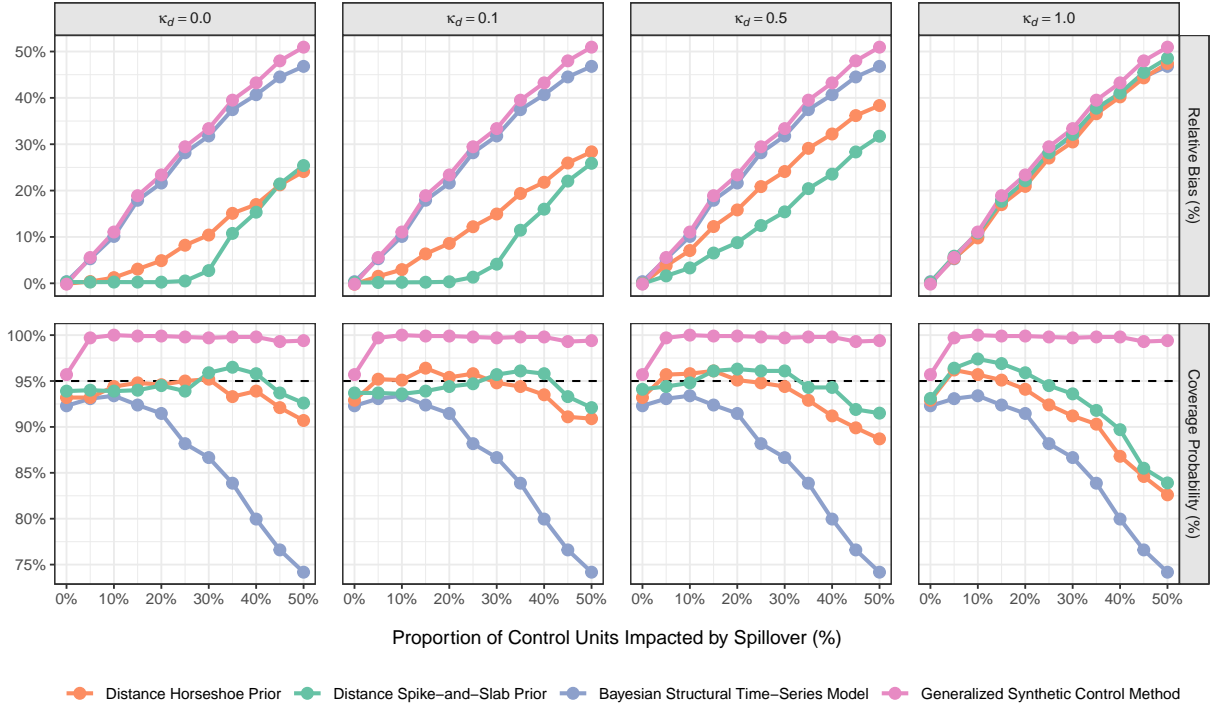


Figure 1: Relative bias (upper) and coverage probability (lower) across 1,000 replicates with $T_0 = 30$ pre-intervention periods and $J = 50$ control units, comparing our distance-based priors to alternative methods. Results are shown for varying values of κ_d and spillover magnitudes. Bias is relative to the true treatment effect ($\tau_t = 7$), while coverage probability is based on 95% credible (or confidence) intervals. The dashed horizontal line denotes the 95% nominal coverage level.

model, in particular, shows undercoverage, likely due to its biased estimates, combined with confidence intervals that are not sufficiently widened to compensate for this bias, leading to difficulties in covering the true intervention effect. On the other hand, the GSC method displays overcoverage, nearing 100%, which may result from its uncertainty estimation approach yielding overly wide confidence intervals.

In the special case where $\kappa_d = 0$, meaning the penalty relies solely on the spatial proximity of control units to the treated unit, our DS2 shows the least bias and maintains approximately nominal coverage up to 40% spillover. Beyond this threshold, it begins to exhibit undercoverage. However, when the cutoff ρ is misspecified (i.e., $\rho < \rho^*$) at spillover levels above 25%, the bias increases, becoming comparable to the DHS, though it remains significantly lower than that of the BSTS and GSC methods. This occurs because ρ underestimates the true spillover in the donor pool, resulting in the DS2 selecting affected controls when building the SC, thereby increasing bias from unaccounted spillover effects. Furthermore, the results for the DS2 at $\kappa_d = 0.0$ and $\kappa_d = 0.1$ are nearly identical, as the weighted distances are likely too similar to exclude different sets of controls from the donor pool. Both priors perform similarly in

terms of relative bias and coverage probability at low and high levels of spillover. However, the DHS prior exhibits slightly higher bias than the DS2 prior at intermediate spillover levels, ranging from 15% to 40%, though both remain significantly less biased than the two alternative methods.

When $\kappa_d = 0.5$, where covariate similarity and spatial proximity are equally weighted, the bias and coverage probability of our proposed methods remain lower and closer to nominal values compared to the two alternative methods, specifically in scenarios without spillovers (e.g., 0%). However, bias increases in the presence of spillovers. This is because selecting controls similar to the treated units can enhance predictive power but also increases the likelihood of spillover bias if controls are spatially close. For both priors, the highest bias occurs when $\kappa_d = 1$, where the penalty is based solely on the dissimilarity between the baseline covariates \mathbf{X}_i of the control units and the treated unit. This leads to a bias nearly identical to the two alternative methods, likely because all are equally impacted by the spillover effect. The findings for $\kappa_d = 1$ come from the distance-based spillover effects in our simulation study, where the priors may select neighboring controls that are similar to the treated unit in terms of \mathbf{X}_i , yet are still influenced by spillover due to their spatial proximity.

We conduct an additional simulation study that accounts for distance-dependent covariate similarities. In this scenario, neighboring controls are far more similar in terms of \mathbf{X}_i than those located farther from the treated unit, highlighting the advantages of incorporating covariate similarity when constructing the SC – either in addition to, or instead of, spatial proximity. In these cases, we can use a higher value of κ_d in our priors to balance the importance of covariate similarity and spatial proximity, a feature lacking in the two alternative methods. Further details about this separate experiment as well as the main simulations, including the data-generating process, finite-sample precision, and root-mean-square error results, are provided in the Supporting Information.

5. Application to Philadelphia’s Beverage Tax

We apply the DHS and DS2 priors in (6) and (7) to evaluate the impact of Philadelphia’s beverage tax, implemented on January 1, 2017, on the sales volume of sugar-sweetened and artificially sweetened beverages in mass-merchandise stores throughout the county. Sales data are sourced from the NielsenIQ Retail Scanner dataset, curated by the Kilts Center at the University of Chicago Booth School of Business (NielsenIQ, 2006). This dataset provides weekly insights into pricing, sales volume, and store

environment details from participating retail chains nationwide.

We analyze data from mass-merchandise retail chains in Pennsylvania and its neighboring states (Delaware, Maryland, and New Jersey) that provided complete sales records for carbonated soft beverages over the full observation period, spanning January 3, 2016, to December 30, 2017. The collected sales volumes, measured in fluid ounces, are aggregated by the three-digit ZIP code (ZIP3) region corresponding to each store’s location. We treat these ZIP3 areas as our units of interest, with Philadelphia entirely contained within one ZIP3 area, which we designate as the treated unit. Next, we aggregate the outcomes (sales volume) into four-week periods and standardize them according to the number of stores in each region, excluding ZIP3 areas located more than 125,000 meters from Philadelphia. This reduction in the size of the donor pool helps avoid potential complications associated with using an excessive number of control units (Abadie et al., 2015; Kinn, 2018). In total, we include $J = 48$ control units (ZIP3 areas) in the donor pool, each with $T = 26$ periods of complete sales data and $T_0 = 13$ pre-tax periods. We calculate the distance from each control to the treated unit based on the Euclidean distance between their geographic centroids. Baseline covariates, including demographic data, income levels, and population density for the selected ZIP3 areas, are obtained from the United States Census Bureau. We use these baseline covariates to compute the weighted distance $d_{i,1}^C$ for various values of $\kappa_d \in \{0.0, 0.1, 0.5, 1.0\}$ in (5). The cutoff ρ in (7) is set to exclude roughly 25% of the donor pool.

We estimate the target estimand τ_t in (1) at each post-intervention time point using the DHS and DS2 priors, for $t = T_0 + 1, \dots, T$. Each time point t represents a four-week interval. This estimand reflects the causal effect of the excise tax on the outcome, specifically the relative volume of sales in Philadelphia. We emphasize that our analysis focuses on evaluating the effect at individual time points, rather than assessing simultaneous effects across multiple periods. For each prior, we run four independent MCMC chains, each with 5,000 iterations, discarding the first 3,000 as burn-in. The hyperparameters for the prior distributions of φ and ϕ are set as follows: $\mu_\varphi = 0$, $\sigma_\varphi = 3$, $\nu_\phi = 4$, and $\tau_\phi = 1$. The baseline covariates are standardized based on their respective mean and variance estimates, while the observed outcomes are standardized using the mean and variance calculated solely from the pre-intervention period.

Figure 2 displays the posterior means and 95% credible intervals of τ_t , for all four-week periods within the observational window and across varying values of κ_d . The pre-intervention period shows a strong model fit, with causal effect estimates consistently centered around zero. Post-intervention results

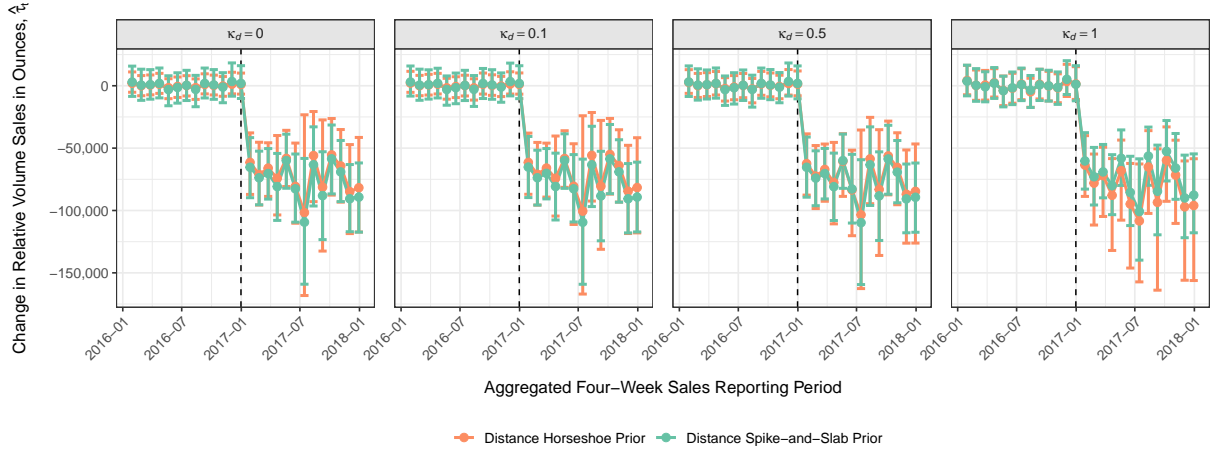


Figure 2: Posterior mean and 95% credible interval pointwise estimates for the effect τ_t of the beverage tax on relative volume sales in Philadelphia, shown across different values of κ_d for both the DHS and DS2. Estimates are calculated for each four-week aggregated period $t \in [T]$. The DS2 prior assumes a cutoff ρ where 25% of the donor pool is affected by spillover. The black dashed line marks the implementation date of the beverage tax in Philadelphia.

indicate a reduction in sales, with all credible intervals for the post-intervention estimates excluding zero, regardless of the κ_d value. The DS2 results remain relatively consistent across different κ_d values, likely because the weighted distances $d_{i,1}^C$ computed for varying κ_d values show minimal differences. In the DHS, the observed greater reduction in beverage sales with increasing κ_d , which applies a stronger penalty for covariate dissimilarity, may result from including neighboring controls more similar to the treated unit. This inclusion may lead to inflated estimates due to spillover bias and greater uncertainty, as reflected in wider credible intervals. Additional exploratory figures related to the application, further details on the analysis, and a sensitivity analysis examining the beverage tax effect estimates across varying spillover percentages associated with ρ are provided in the Supporting Information.

6. Discussion

This work introduces distance-based shrinkage priors designed to estimate intervention effects in scenarios where spillover occurs. We extend conventional Bayesian penalization techniques by developing the DHS and DS2 priors, which are specifically formulated to data-adaptively select control units that are less likely to be impacted by spillover. Central to our approach is a weighted distance function that adjusts the shrinkage of the SC coefficients when applying our priors. This function is a convex combination of each unit’s covariate dissimilarity and its spatial proximity to the treated unit. While we primarily use

Euclidean distance to measure spatial proximity, our framework allows for the incorporation of alternative distance metrics to accommodate different contexts. Through extensive simulation studies, we show that our priors offer more favorable finite-sample properties compared to other alternative methods, especially as the proportion of the donor pool impacted by spillover increases. Although we focus on policy evaluation, our methodology is broadly applicable to any field where the comparison groups may be indirectly affected by spillover from an intervention or treatment.

Our work acknowledges some limitations. First, the cutoff ρ used in the DS2 is a crucial hyperparameter that affects the performance of the Bayesian SC estimator. Our simulation studies indicate that misspecifying ρ (e.g., when the proportion of control units impacted by spillover is far higher than ρ) can result in higher bias. To address this, given the contexts, we recommend setting ρ more liberally to include a larger portion of the donor pool. Although this approach may exclude some valid control units unaffected by the intervention, potentially reducing the predictive power of the SC and increasing the estimator's variance, the impact on bias is generally minimal, provided the donor pool is sufficiently large. On the other hand, including control units that are potentially affected by spillovers can easily induce bias. Second, in our data application study, using ZIP3 areas instead of standard seven-digit ZIP code (ZIP7) areas introduces some limitations. ZIP3 areas encompass larger and more diverse neighborhoods, which can lead to cruder demographic and socio-economic data, potentially reducing the detail and precision of the analysis. Aggregating data over these broader areas might either amplify or diminish spillover effects, affecting the accuracy of the results. On the other hand, using ZIP7 areas as units complicates the intervention's assignment. This is due to Philadelphia and its surrounding counties containing multiple ZIP7 areas, leading to several spatially close units being assigned the intervention. This setup may require alternative approaches that allow for multiple treated units and correlated intervention assignments.

Finally, our primary methodology focuses on the horseshoe and spike-and-slab penalization techniques, given their widespread use in statistical applications and their flexibility in adjusting shrinkage through hyperparameters or secondary data. Future research could expand this approach by exploring additional conventional penalization methods and investigating alternative shrinkage priors, such as Dirichlet-Laplace or Laplace priors, which may offer different criteria for selecting controls. Further modifications could extend this framework to accommodate non-continuous or non-normal data, such as discrete or non-negative outcomes, which may require alternative distributions like Poisson or Gamma. Additionally, the

framework could be adapted to handle multiple treated units by specifying a multivariate distribution with unit-specific SC coefficients, potentially using a common prior with a distance-dependent hyperprior. Given these potential extensions, our work seeks to foster discussion and initiate methodological advancements in evaluating policy interventions involving controls potentially impacted by spillovers.

Acknowledgements

This material is based upon work supported by the National Science Foundation Graduate Research Fellowship under Grant No. 2040433. Any opinion, findings, and conclusions or recommendations expressed in this material are those of the authors and do not necessarily reflect the views of the National Science Foundation. Funding for Dr. Youjin Lee was provided by the National Institute of Diabetes and Digestive and Kidney Diseases through award R01DK136515.

Data Availability Statement

Researchers' own analyses derived based in part on data from Nielsen Consumer LLC and marketing databases provided through the NielsenIQ Datasets at the Kilts Center for Marketing Data Center at The University of Chicago Booth School of Business. The conclusions drawn from the NielsenIQ data are those of the researchers and do not reflect the views of NielsenIQ. NielsenIQ is not responsible for, had no role in, and was not involved in analyzing and preparing the results reported herein.

References

- Abadie, A., Diamond, A., and Hainmueller, J. (2010). Synthetic Control Methods for Comparative Case Studies: Estimating the Effect of California's Tobacco Control Program. *Journal of the American Statistical Association* **105**, 493–505.
- Abadie, A., Diamond, A., and Hainmueller, J. (2015). Comparative Politics and the Synthetic Control Method: COMPARATIVE POLITICS AND THE SYNTHETIC CONTROL METHOD. *American Journal of Political Science* **59**, 495–510.
- Abadie, A. and Gardeazabal, J. (2003). The Economic Costs of Conflict: A Case Study of the Basque Country. *American Economic Review* **93**, 113–132.

- Ashenfelter, O. (1978). Estimating the Effect of Training Programs on Earnings. *The Review of Economics and Statistics* **60**, 47.
- Ashenfelter, O. and Card, D. (1984). Using the Longitudinal Structure of Earnings to Estimate the Effect of Training Programs. Technical Report w1489, National Bureau of Economic Research, Cambridge, MA.
- Brodersen, K. H., Gallusser, F., Koehler, J., Remy, N., and Scott, S. L. (2015). Inferring causal impact using Bayesian structural time-series models. *The Annals of Applied Statistics* **9**,.
- Butts, K. (2023). Difference-in-Differences Estimation with Spatial Spillovers. arXiv:2105.03737 [econ].
- Cao, J. and Dowd, C. (2019). Estimation and Inference for Synthetic Control Methods with Spillover Effects. arXiv:1902.07343 [econ].
- Carpenter, B., Gelman, A., Hoffman, M. D., Lee, D., Goodrich, B., Betancourt, M., Brubaker, M., Guo, J., Li, P., and Riddell, A. (2017). *Stan* : A Probabilistic Programming Language. *Journal of Statistical Software* **76**,.
- Carvalho, C. M., Polson, N. G., and Scott, J. G. (2010). The horseshoe estimator for sparse signals. *Biometrika* **97**, 465–480.
- Di Stefano, R. and Mellace, G. (2024). The inclusive Synthetic Control Method. arXiv:2403.17624 [econ].
- George, E. I. and McCulloch, R. E. (1993). Variable Selection via Gibbs Sampling. *Journal of the American Statistical Association* **88**, 881–889.
- Grossi, G., Mariani, M., Mattei, A., Lattarulo, P., and Öner, Ö. (2024). Direct and spillover effects of a new tramway line on the commercial vitality of peripheral streets: a synthetic-control approach. *Journal of the Royal Statistical Society Series A: Statistics in Society* page qnae032.
- Hastings, W. K. (1970). Monte Carlo sampling methods using Markov chains and their applications. *Biometrika* **57**, 97–109.
- Hettinger, G., Roberto, C., Lee, Y., and Mitra, N. (2023). Estimation of Policy-Relevant Causal Effects in the Presence of Interference with an Application to the Philadelphia Beverage Tax. Version Number: 2.

- Holland, P. W. (1986). Statistics and Causal Inference. *Journal of the American Statistical Association* **81**, 945–960.
- Jaccard, P. (1912). THE DISTRIBUTION OF THE FLORA IN THE ALPINE ZONE. ¹. *New Phytologist* **11**, 37–50.
- Kim, S., Lee, C., and Gupta, S. (2020). Bayesian Synthetic Control Methods. *Journal of Marketing Research* **57**, 831–852.
- Kinn, D. (2018). Synthetic Control Methods and Big Data. arXiv:1803.00096 [econ].
- Lee, Y., Hettinger, G., and Mitra, N. (2023). Policy effect evaluation under counterfactual neighborhood interventions in the presence of spillover. arXiv:2303.06227 [stat].
- Li, F., Ding, P., and Mealli, F. (2023). Bayesian causal inference: a critical review. *Philosophical Transactions of the Royal Society A: Mathematical, Physical and Engineering Sciences* **381**, 20220153.
- Li, K. T. (2020). Statistical Inference for Average Treatment Effects Estimated by Synthetic Control Methods. *Journal of the American Statistical Association* **115**, 2068–2083.
- Mahalanobis, P. C. (1936). On the Generalized Distance in Statistics. *Proceedings of the National Institute of Sciences of India* **2**, 49–55. Publisher: National Institute of Sciences of India.
- Marinello, S., Leider, J., Pugach, O., and Powell, L. M. (2021). The impact of the Philadelphia beverage tax on employment: A synthetic control analysis. *Economics & Human Biology* **40**, 100939.
- Mitchell, T. J. and Beauchamp, J. J. (1988). Bayesian Variable Selection in Linear Regression. *Journal of the American Statistical Association* **83**, 1023–1032.
- NielsenIQ (2006). Retail Scanner Data.
- Oganisian, A. and Roy, J. A. (2021). A practical introduction to Bayesian estimation of causal effects: Parametric and nonparametric approaches. *Statistics in Medicine* **40**, 518–551.
- Pang, X., Liu, L., and Xu, Y. (2022). A Bayesian Alternative to Synthetic Control for Comparative Case Studies. *Political Analysis* **30**, 269–288.
- Piironen, J. and Vehtari, A. (2017). Sparsity information and regularization in the horseshoe and other shrinkage priors. *Electronic Journal of Statistics* **11**,

- Robert, C. P. (2015). The Metropolis–Hastings Algorithm. In Kenett, R. S., Longford, N. T., Piegorsch, W. W., and Ruggeri, F., editors, *Wiley StatsRef: Statistics Reference Online*, pages 1–15. Wiley, 1 edition.
- Roberto, C. A., Lawman, H. G., LeVasseur, M. T., Mitra, N., Peterhans, A., Herring, B., and Bleich, S. N. (2019). Association of a Beverage Tax on Sugar-Sweetened and Artificially Sweetened Beverages With Changes in Beverage Prices and Sales at Chain Retailers in a Large Urban Setting. *JAMA* **321**, 1799.
- Rubin, D. B. (1974). Estimating causal effects of treatments in randomized and nonrandomized studies. *Journal of Educational Psychology* **66**, 688–701.
- Rubin, D. B. (1980). Randomization Analysis of Experimental Data: The Fisher Randomization Test Comment. *Journal of the American Statistical Association* **75**, 591.
- Verbitsky-Savitz, N. and Raudenbush, S. W. (2012). Causal Inference Under Interference in Spatial Settings: A Case Study Evaluating Community Policing Program in Chicago. *Epidemiologic Methods* **1**,
- Wu, G., Boateng, F. D., and Lang, X. (2020). The Spillover Effect of Recreational Marijuana Legalization on Crime: Evidence From Neighboring States of Colorado and Washington State. *Journal of Drug Issues* **50**, 392–409.
- Xu, Y. (2017). Generalized Synthetic Control Method: Causal Inference with Interactive Fixed Effects Models. *Political Analysis* **25**, 57–76.

Supporting Information

Web Appendices, Tables, and Figures referenced in Sections 2, 3, 4, and 5 are available with this paper online. Code used in simulations and data analysis can be found in the first author’s GitHub at <https://github.com/estfernan/Shrinkage-Priors-Spillover-SC>. Example data that resembles the structure of the Retail Scanner data is also provided for illustration, as the original used in this study is not publicly accessible.

Web Appendix A. Proofs and Auxiliary Results

Web Appendix A.1 *Proof of posterior predictive distribution*

We derive the posterior predictive distribution (PPD) under the assumption that there are only two post-intervention periods, $T = T_0 + 2$, where the following proof can be generalized to settings with more than two. Let $\mathbf{Y}^m = (Y_{1(T_0+1)}(\mathbf{0}_n), Y_{1(T_0+2)}(\mathbf{0}_n))$ be the (missing) post-intervention potential outcomes, with the set of observed data $\mathbf{O} = (\bar{\mathbf{V}}_T, \bar{Y}_{1T_0}, \bar{\mathbf{Z}}_{T_0} = \bar{\mathbf{0}}_n)$ and baseline covariates \mathbf{X} . The PPD for \mathbf{Y}^m , conditioned on \mathbf{O} and \mathbf{X} , can be expressed as

$$p(\mathbf{Y}^m \mid \mathbf{O}, \mathbf{X}) = p(\mathbf{Y}^m, \mathbf{O} \mid \mathbf{X}) / p(\mathbf{O} \mid \mathbf{X}) \propto p(\mathbf{Y}^m, \mathbf{O} \mid \mathbf{X}),$$

where $p(\mathbf{O} \mid \mathbf{X})$ is absorbed by the proportionality constant. Under de Finetti's theorem, we introduce a set of parameters $\boldsymbol{\theta} \in \Theta$ that govern the joint distribution of \mathbf{Y}^m and \mathbf{O} , with Θ being the parameter space. Therefore, the PPD can be given by

$$p(\mathbf{Y}^m \mid \mathbf{O}, \mathbf{X}) \propto \int_{\Theta} p(\mathbf{Y}^m, \mathbf{O} \mid \mathbf{X}, \boldsymbol{\theta}) \pi(\boldsymbol{\theta} \mid \mathbf{X}) d\boldsymbol{\theta},$$

where the joint distribution of \mathbf{Y}^m and \mathbf{O} can be further expressed as

$$p(\mathbf{Y}^m, \mathbf{O} \mid \mathbf{X}, \boldsymbol{\theta}) = p(\mathbf{Y}^m \mid \mathbf{O}, \mathbf{X}, \boldsymbol{\theta}) p(\mathbf{O} \mid \mathbf{X}, \boldsymbol{\theta}).$$

Here, we need to identify the distribution of \mathbf{Y}^m , denoted by $p(\mathbf{Y}^m \mid \mathbf{O}, \mathbf{X}, \boldsymbol{\theta})$, in terms of imputable or observable quantities. Likewise, the observed data distribution (likelihood) is represented by $p(\mathbf{O} \mid \mathbf{X}, \boldsymbol{\theta})$ and is derived in the subsequent section. Under Assumptions 1-3, outlined in the main text, we can start

identifying $p(\mathbf{Y}^m \mid \mathbf{O}, \mathbf{X}, \boldsymbol{\theta})$ as follows:

$$\begin{aligned}
p(\mathbf{Y}^m \mid \mathbf{O}, \mathbf{X}, \boldsymbol{\theta}) &\stackrel{\text{(E1)}}{=} p(Y_{1(T_0+1)}(\mathbf{O}_n), Y_{1(T_0+2)}(\mathbf{O}_n) \mid \bar{\mathbf{V}}_T, \bar{Y}_{1T_0}, \bar{\mathbf{Z}}_{T_0} = \bar{\mathbf{0}}_n, \mathbf{X}, \boldsymbol{\theta}) \\
&= p(Y_{1(T_0+1)}(\mathbf{O}_n), Y_{1(T_0+2)}(\mathbf{O}_n) \mid \mathbf{V}_{T_0+2}, \bar{\mathbf{V}}_{T_0+1}, \bar{Y}_{1T_0}, \bar{\mathbf{Z}}_{T_0} = \bar{\mathbf{0}}_n, \mathbf{X}, \boldsymbol{\theta}) \\
&\stackrel{\text{(E2)}}{=} p(Y_{1(T_0+1)}(\mathbf{O}_n), Y_{1(T_0+2)}(\mathbf{O}_n) \mid \mathbf{V}_{T_0+2}, \bar{\mathbf{V}}_{T_0+1}, \bar{Y}_{1T_0}, \bar{\mathbf{Z}}_{T_0} = \bar{\mathbf{0}}_n, \boldsymbol{\theta}) \\
&\stackrel{\text{(E3)}}{=} p(Y_{1(T_0+1)}(\mathbf{O}_n), Y_{1(T_0+2)}(\mathbf{O}_n) \mid \mathbf{V}_{T_0+2}, \mathbf{Z}_{T_0+1} = \mathbf{0}_n, \bar{\mathbf{V}}_{T_0+1}, \bar{Y}_{1T_0}, \bar{\mathbf{Z}}_{T_0} = \bar{\mathbf{0}}_n, \boldsymbol{\theta}) \\
&\stackrel{\text{(E4)}}{=} p(Y_{1(T_0+1)}, Y_{1(T_0+2)}(\mathbf{O}_n) \mid \mathbf{V}_{T_0+2}, \mathbf{Z}_{T_0+1} = \mathbf{0}_n, \bar{\mathbf{V}}_{T_0+1}, \bar{Y}_{1T_0}, \bar{\mathbf{Z}}_{T_0} = \bar{\mathbf{0}}_n, \boldsymbol{\theta}) \\
&= p(Y_{1(T_0+1)}, Y_{1(T_0+2)}(\mathbf{O}_n) \mid \mathbf{V}_{T_0+2}, \bar{\mathbf{Z}}_{T_0+1} = \bar{\mathbf{0}}_n, \bar{\mathbf{V}}_{T_0+1}, \bar{Y}_{1T_0}, \boldsymbol{\theta}).
\end{aligned}$$

Equality (E1) follows from the variable definitions of \mathbf{Y}^m and \mathbf{O} . Under Assumption 3, Equalities (E2) and (E3) are justified by covariate independence and sequential ignorability. Finally, Assumption 2 upholds Equality (E4) by linking the potential outcome to an imputable quantity through consistency. Following this result, the joint distribution of $Y_{1(T_0+1)}$ and $Y_{1(T_0+2)}(\mathbf{O}_n)$ can be expressed as

$$\begin{aligned}
&p(Y_{1(T_0+1)}, Y_{1(T_0+2)}(\mathbf{O}_n) \mid \mathbf{V}_{T_0+2}, \bar{\mathbf{Z}}_{T_0+1} = \bar{\mathbf{0}}_n, \bar{\mathbf{V}}_{T_0+1}, \bar{Y}_{1T_0}, \boldsymbol{\theta}) \\
&= p(Y_{1(T_0+2)}(\mathbf{O}_n) \mid \mathbf{V}_{T_0+2}, Y_{1(T_0+1)}, \bar{\mathbf{Z}}_{T_0+1} = \bar{\mathbf{0}}_n, \bar{\mathbf{V}}_{T_0+1}, \bar{Y}_{1T_0}, \boldsymbol{\theta}) \\
&\quad \times p(Y_{1(T_0+1)} \mid \mathbf{V}_{T_0+2}, \bar{\mathbf{Z}}_{T_0+1} = \bar{\mathbf{0}}_n, \bar{\mathbf{V}}_{T_0+1}, \bar{Y}_{1T_0}, \boldsymbol{\theta}) \\
&\stackrel{\text{(E5)}}{=} p(Y_{1(T_0+2)}(\mathbf{O}_n) \mid \mathbf{V}_{T_0+2}, Y_{1(T_0+1)}, \bar{\mathbf{Z}}_{T_0+1} = \bar{\mathbf{0}}_n, \bar{\mathbf{V}}_{T_0+1}, \bar{Y}_{1T_0}, \boldsymbol{\theta}) \\
&\quad \times p(Y_{1(T_0+1)} \mid \bar{\mathbf{Z}}_{T_0+1} = \bar{\mathbf{0}}_n, \bar{\mathbf{V}}_{T_0+1}, \bar{Y}_{1T_0}, \boldsymbol{\theta}) \\
&= p(Y_{1(T_0+2)}(\mathbf{O}_n) \mid \bar{\mathbf{V}}_{T_0+2}, \bar{Y}_{1(T_0+1)}, \bar{\mathbf{Z}}_{T_0+1} = \bar{\mathbf{0}}_n, \boldsymbol{\theta}) \\
&\quad \times p(Y_{1(T_0+1)} \mid \bar{\mathbf{Z}}_{T_0+1} = \bar{\mathbf{0}}_n, \bar{\mathbf{V}}_{T_0+1}, \bar{Y}_{1T_0}, \boldsymbol{\theta}).
\end{aligned}$$

Equality (E5) follows from the assumption that future observations, \mathbf{V}_{T_0+2} , do not impact previous outcomes, $Y_{1(T_0+1)}$. Under Assumptions 1-3, we take an identical approach to identify the distribution of

$Y_{1(T_0+2)}(\mathbf{0}_n)$ as follows:

$$\begin{aligned}
& p(Y_{1(T_0+2)}(\mathbf{0}_n) \mid \bar{\mathbf{V}}_{T_0+2}, \bar{Y}_{1(T_0+1)}, \bar{\mathbf{Z}}_{T_0+1} = \bar{\mathbf{0}}_n, \boldsymbol{\theta}) \\
& \stackrel{\text{(E6)}}{=} p(Y_{1(T_0+2)}(\mathbf{0}_n) \mid \mathbf{Z}_{T_0+2} = \mathbf{0}_n, \bar{\mathbf{V}}_{T_0+2}, \bar{Y}_{1(T_0+1)}, \bar{\mathbf{Z}}_{T_0+1} = \bar{\mathbf{0}}_n, \boldsymbol{\theta}) \\
& \stackrel{\text{(E7)}}{=} p(Y_{1(T_0+2)} \mid \mathbf{Z}_{T_0+2} = \mathbf{0}_n, \bar{\mathbf{V}}_{T_0+2}, \bar{Y}_{1(T_0+1)}, \bar{\mathbf{Z}}_{T_0+1} = \bar{\mathbf{0}}_n, \boldsymbol{\theta}) \\
& = p(Y_{1(T_0+2)} \mid \bar{\mathbf{Z}}_{T_0+2} = \bar{\mathbf{0}}_n, \bar{\mathbf{V}}_{T_0+2}, \bar{Y}_{1(T_0+1)}, \boldsymbol{\theta}),
\end{aligned}$$

where Equalities (E6) and (E7) hold under sequential ignorability, followed by consistency. We note that the final expression for $p(\mathbf{Y}^m \mid \mathbf{O}, \mathbf{X}, \boldsymbol{\theta})$ can be written as a product of conditional distributions, such that

$$p(\mathbf{Y}^m \mid \mathbf{O}, \mathbf{X}, \boldsymbol{\theta}) = \prod_{t>T_0} p(Y_{1t} \mid \bar{\mathbf{Z}}_t = \bar{\mathbf{0}}_n, \bar{\mathbf{V}}_t, \bar{Y}_{1(t-1)}, \boldsymbol{\theta}).$$

Subsequently, the PPD can be currently expressed as

$$\begin{aligned}
p(\mathbf{Y}^m \mid \mathbf{O}, \mathbf{X}) & \propto \int_{\Theta} p(\mathbf{Y}^m \mid \mathbf{O}, \mathbf{X}, \boldsymbol{\theta}) p(\mathbf{O} \mid \mathbf{X}, \boldsymbol{\theta}) \pi(\boldsymbol{\theta} \mid \mathbf{X}) d\boldsymbol{\theta} \\
& = \int_{\Theta} \prod_{t>T_0} p(Y_{1t} \mid \bar{\mathbf{Z}}_t = \bar{\mathbf{0}}_n, \bar{\mathbf{V}}_t, \bar{Y}_{1(t-1)}, \boldsymbol{\theta}) p(\mathbf{O} \mid \mathbf{X}, \boldsymbol{\theta}) \pi(\boldsymbol{\theta} \mid \mathbf{X}) d\boldsymbol{\theta}.
\end{aligned}$$

In the following sections, we derive expressions for both $p(\mathbf{O} \mid \mathbf{X}, \boldsymbol{\theta})$ and $\pi(\boldsymbol{\theta} \mid \mathbf{X})$.

Web Appendix A.2 *Derivation of Observed Data Distribution*

Under Assumption 1, we do not need to identify $p(\mathbf{O} \mid \mathbf{X}, \boldsymbol{\theta})$ since $Y_{1t} = Y_{1t}(\mathbf{0}_n)$ for all $t \leq T_0$.

Furthermore, using the longitudinal dependence of the observations, we can express the observed data distribution as a product of distributions:

$$\begin{aligned}
& p(\mathbf{O} \mid \mathbf{X}, \boldsymbol{\theta}) \\
& = p(\bar{\mathbf{V}}_T, \bar{Y}_{1T_0}, \bar{\mathbf{Z}}_{T_0} = \bar{\mathbf{0}}_n \mid \mathbf{X}, \boldsymbol{\theta}) \\
& = p(\underline{\mathbf{V}}_{T_0+1} \mid \bar{\mathbf{V}}_{T_0}, \bar{Y}_{1T_0}, \bar{\mathbf{Z}}_{T_0} = \bar{\mathbf{0}}_n, \mathbf{X}, \boldsymbol{\theta}) \prod_{t \leq T_0} p(\mathbf{V}_t, Y_{1t}, \mathbf{Z}_t = \mathbf{0}_n \mid \bar{\mathbf{V}}_{t-1}, \bar{Y}_{1(t-1)}, \bar{\mathbf{Z}}_{t-1} = \bar{\mathbf{0}}_n, \mathbf{X}, \boldsymbol{\theta}).
\end{aligned}$$

Recall that our parameter of interest $\boldsymbol{\theta}$ solely governs the distribution of Y_{1t} . Therefore, the distribution of \mathbf{V}_{T_0+1} can be absorbed into the proportionality constant:

$$p(\mathbf{O} \mid \mathbf{X}, \boldsymbol{\theta}) \propto \prod_{t \leq T_0} p(\mathbf{V}_t, Y_{1t}, \mathbf{Z}_t = \mathbf{0}_n \mid \bar{\mathbf{V}}_{t-1}, \bar{Y}_{1(t-1)}, \bar{\mathbf{Z}}_{t-1} = \bar{\mathbf{0}}_n, \mathbf{X}, \boldsymbol{\theta}).$$

Here, the joint distribution of \mathbf{V}_t , Y_{1t} , and $\mathbf{Z}_t = \mathbf{0}_n$ can be expressed as

$$\begin{aligned} & p(\mathbf{V}_t, Y_{1t}, \mathbf{Z}_t = \bar{\mathbf{0}}_n \mid \bar{\mathbf{V}}_{t-1}, \bar{Y}_{1(t-1)}, \bar{\mathbf{Z}}_{t-1} = \bar{\mathbf{0}}_n, \mathbf{X}, \boldsymbol{\theta}) \\ &= p(\mathbf{V}_t, \mathbf{Z}_t = \bar{\mathbf{0}}_n \mid \bar{\mathbf{V}}_{t-1}, \bar{Y}_{1(t-1)}, \bar{\mathbf{Z}}_{t-1} = \bar{\mathbf{0}}_n, \mathbf{X}, \boldsymbol{\theta}) \\ &\quad \times p(Y_{1t} \mid \mathbf{V}_t, \mathbf{Z}_t = \bar{\mathbf{0}}_n, \bar{\mathbf{V}}_{t-1}, \bar{Y}_{1(t-1)}, \bar{\mathbf{Z}}_{t-1} = \bar{\mathbf{0}}_n, \mathbf{X}, \boldsymbol{\theta}) \\ &= p(\mathbf{V}_t, \mathbf{Z}_t = \bar{\mathbf{0}}_n \mid \bar{\mathbf{V}}_{t-1}, \bar{Y}_{1(t-1)}, \bar{\mathbf{Z}}_{t-1} = \bar{\mathbf{0}}_n, \mathbf{X}, \boldsymbol{\theta}) \\ &\quad \times p(Y_{1t} \mid \bar{\mathbf{Z}}_t = \bar{\mathbf{0}}_n, \bar{\mathbf{V}}_t, \bar{Y}_{1(t-1)}, \mathbf{X}, \boldsymbol{\theta}). \end{aligned}$$

Similarly, the joint distribution \mathbf{V}_t and $\mathbf{Z}_t = \bar{\mathbf{0}}_n$ can also be absorbed into the proportionality constant:

$$\begin{aligned} & p(\mathbf{V}_t, Y_{1t}, \mathbf{Z}_t = \bar{\mathbf{0}}_n \mid \bar{\mathbf{V}}_{t-1}, \bar{Y}_{1(t-1)}, \bar{\mathbf{Z}}_{t-1} = \bar{\mathbf{0}}_n, \mathbf{X}, \boldsymbol{\theta}) \\ &\quad \propto p(Y_{1t} \mid \bar{\mathbf{Z}}_t = \bar{\mathbf{0}}_n, \bar{\mathbf{V}}_t, \bar{Y}_{1(t-1)}, \mathbf{X}, \boldsymbol{\theta}). \end{aligned}$$

Therefore, the observed data distribution is given by

$$\begin{aligned} p(\mathbf{O} \mid \mathbf{X}, \boldsymbol{\theta}) &\propto \prod_{t \leq T_0} p(\mathbf{V}_t, Y_{1t}, \mathbf{Z}_t = \mathbf{0}_n \mid \bar{\mathbf{V}}_{t-1}, \bar{Y}_{1(t-1)}, \bar{\mathbf{Z}}_{t-1} = \bar{\mathbf{0}}_n, \mathbf{X}, \boldsymbol{\theta}) \\ &\propto \prod_{t \leq T_0} p(Y_{1t} \mid \bar{\mathbf{Z}}_t = \bar{\mathbf{0}}_n, \bar{\mathbf{V}}_t, \bar{Y}_{1(t-1)}, \mathbf{X}, \boldsymbol{\theta}) \\ &\stackrel{\text{(E8)}}{=} \prod_{t \leq T_0} p(Y_{1t} \mid \bar{\mathbf{Z}}_t = \bar{\mathbf{0}}_n, \bar{\mathbf{V}}_t, \bar{Y}_{1(t-1)}, \boldsymbol{\theta}), \end{aligned}$$

where Equality (E8) follows from covariate independence of Y_{1t} , given the observed history. Subsequently, the PPD can be currently expressed as

$$\begin{aligned} p(\mathbf{Y}^m \mid \mathbf{O}, \mathbf{X}) &\propto \int_{\Theta} \prod_{t > T_0} p(Y_{1t} \mid \bar{\mathbf{Z}}_t = \bar{\mathbf{0}}_n, \bar{\mathbf{V}}_t, \bar{Y}_{1(t-1)}, \boldsymbol{\theta}) p(\mathbf{O} \mid \mathbf{X}, \boldsymbol{\theta}) \pi(\boldsymbol{\theta} \mid \mathbf{X}) d\boldsymbol{\theta} \\ &\propto \int_{\Theta} \prod_{t > T_0} p(Y_{1t} \mid \bar{\mathbf{Z}}_t = \bar{\mathbf{0}}_n, \bar{\mathbf{V}}_t, \bar{Y}_{1(t-1)}, \boldsymbol{\theta}) \prod_{t \leq T_0} p(Y_{1t} \mid \bar{\mathbf{Z}}_t = \bar{\mathbf{0}}_n, \bar{\mathbf{V}}_t, \bar{Y}_{1(t-1)}, \boldsymbol{\theta}) \pi(\boldsymbol{\theta} \mid \mathbf{X}) d\boldsymbol{\theta}. \end{aligned}$$

Web Appendix A.3 *Derivation of Prior and Posterior Distributions*

The following derivations are model-specific, based on the details given in the main text. Recall that $\boldsymbol{\theta} = (\boldsymbol{\beta}, \varphi, \phi)$, where its distribution can be given by

$$\pi(\boldsymbol{\theta} \mid \mathbf{X}) = \pi(\boldsymbol{\beta}, \varphi, \phi \mid \mathbf{X}).$$

We assume that φ and ϕ are distinct parameters, independent of each other, as well as of \mathbf{X} . From the model specification, we note that $\boldsymbol{\beta}$ does not depend on φ . Additionally, we introduce a set of hyperparameters $\boldsymbol{\gamma} \in \Gamma$ that fully or partially govern the distribution of $\boldsymbol{\beta}$, with Γ denoting the parameter space. Therefore, we can express $\pi(\boldsymbol{\theta} \mid \mathbf{X})$ as

$$\begin{aligned} \pi(\boldsymbol{\theta} \mid \mathbf{X}) &= \pi(\boldsymbol{\beta}, \varphi, \phi \mid \mathbf{X}) \\ &= \pi(\varphi, \phi \mid \mathbf{X})\pi(\boldsymbol{\beta} \mid \mathbf{X}, \varphi, \phi) \\ &\stackrel{\text{(E9)}}{=} \pi(\varphi)\pi(\phi)\pi(\boldsymbol{\beta} \mid \mathbf{X}, \phi) \\ &\stackrel{\text{(E10)}}{=} \pi(\varphi)\pi(\phi) \int_{\Gamma} \pi(\boldsymbol{\beta} \mid \mathbf{X}, \phi, \boldsymbol{\gamma})\pi(\boldsymbol{\gamma} \mid \mathbf{X})d\boldsymbol{\gamma}. \end{aligned}$$

Equality (E9) follows from the independence assumptions on φ , ϕ , and $\boldsymbol{\beta}$, while Equality (E10) introduces the hyperparameters by marginalizing the distribution of $\boldsymbol{\beta}$, conditional on $\boldsymbol{\gamma}$. Under the assumption that $\boldsymbol{\beta}$ is independent of \mathbf{X} , given $\boldsymbol{\gamma}$, we obtain the following:

$$\begin{aligned} \pi(\boldsymbol{\theta} \mid \mathbf{X}) &= \pi(\varphi)\pi(\phi) \int_{\Gamma} \pi(\boldsymbol{\beta} \mid \mathbf{X}, \phi, \boldsymbol{\gamma})\pi(\boldsymbol{\gamma} \mid \mathbf{X})d\boldsymbol{\gamma} \\ &\stackrel{\text{(E11)}}{=} \pi(\varphi)\pi(\phi) \int_{\Gamma} \pi(\boldsymbol{\beta} \mid \phi, \boldsymbol{\gamma})\pi(\boldsymbol{\gamma} \mid \mathbf{X})d\boldsymbol{\gamma}, \end{aligned}$$

where Equality (E11) stems from this independence assumption. The final expression for the PPD is

$$\begin{aligned} p(\mathbf{Y}^m \mid \mathbf{O}, \mathbf{X}) &\propto \int_{\Theta} \int_{\Gamma} \prod_{t>T_0} p(Y_{1t} \mid \bar{\mathbf{Z}}_t = \bar{\mathbf{0}}_n, \bar{\mathbf{V}}_t, \bar{Y}_{1(t-1)}, \boldsymbol{\theta}) \\ &\quad \times \prod_{t \leq T_0} p(Y_{1t} \mid \bar{\mathbf{Z}}_t = \bar{\mathbf{0}}_n, \bar{\mathbf{V}}_t, \bar{Y}_{1(t-1)}, \boldsymbol{\theta}) \pi(\varphi)\pi(\phi)\pi(\boldsymbol{\beta} \mid \phi, \boldsymbol{\gamma})\pi(\boldsymbol{\gamma} \mid \mathbf{X})d\boldsymbol{\gamma}d\boldsymbol{\theta}. \end{aligned}$$

In the main text, we give the following expression:

$$p(\mathbf{Y}^m | \mathbf{O}, \mathbf{X}) \propto \int_{\Theta} \prod_{t > T_0} p(Y_{1t} | \bar{\mathbf{Z}}_t = \bar{\mathbf{0}}_n, \bar{\mathbf{V}}_t, \bar{Y}_{1(t-1)}, \boldsymbol{\theta}) \pi(\boldsymbol{\theta} | \mathbf{O}, \mathbf{X}) d\boldsymbol{\theta},$$

where $\pi(\boldsymbol{\theta} | \mathbf{O}, \mathbf{X})$ denotes the posterior distribution of $\boldsymbol{\theta}$, given by

$$\begin{aligned} \pi(\boldsymbol{\theta} | \mathbf{O}, \mathbf{X}) &\propto \prod_{t \leq T_0} p(Y_{1t} | \bar{\mathbf{Z}}_t = \bar{\mathbf{0}}_n, \bar{\mathbf{V}}_t, \bar{Y}_{1(t-1)}, \boldsymbol{\theta}) \pi(\varphi) \pi(\phi) \pi(\boldsymbol{\beta} | \mathbf{X}, \phi), \\ \pi(\boldsymbol{\beta} | \mathbf{X}, \phi) &= \int_{\Gamma} \pi(\boldsymbol{\beta} | \phi, \boldsymbol{\gamma}) \pi(\boldsymbol{\gamma} | \mathbf{X}) d\boldsymbol{\gamma}. \end{aligned}$$

Posterior sampling is carried out using Stan (Carpenter et al., 2017), where each component can be individually defined based on the model specification. This procedure allows us to iteratively impute \mathbf{Y}^m by sampling for $\boldsymbol{\theta}$ and $\boldsymbol{\gamma}$, given the observed data \mathbf{O} and \mathbf{X} .

Web Appendix B. Key Notations and Bayesian Networks

Web Table 1 summarizes the key notations of the distance-based horseshoe (DHS) prior and distance-based spike-and-slab (DS2) prior. Web Figures 1 and 2 present the two graphical representations of the outcome model with both the DHS and DS2 priors, respectively. Refer to the main text for a detailed description of the model and its parameters.

Web Appendix C. Additional Simulation Details and Results

Recall, that the linear three-factor model for the potential outcomes in the absence of the intervention, $Y_{it}(\mathbf{0}_n)$, is given by $Y_{it}(\mathbf{0}_n) = \delta_t + \boldsymbol{\vartheta}^T \mathbf{X}_i + \mathbf{f}_t^T \boldsymbol{\mu}_i + \epsilon_{it}$, for $i \in [n]$, $t \in [T]$. In this model, $\delta_t \in \mathbb{R}$ represents a common factor with constant loadings across units, $\boldsymbol{\vartheta} = (\vartheta_1, \vartheta_2) \in \mathbb{R}^2$ is a vector of baseline covariate effects, $\mathbf{f}_t = (f_{1t}, f_{2t}, f_{3t}) \in \mathbb{R}^3$ is a vector of time-varying common factors, $\boldsymbol{\mu}_i = (\mu_{i1}, \mu_{i2}, \mu_{i3}) \in \mathbb{R}^3$ is a vector of factor loadings, and $\epsilon_{it} \in \mathbb{R}$ represents an unobserved transitory shock.

Web Table 2 details the data-generating parameters in the main text. These are set to fixed values throughout the experiments, either pre-specified or generated within each replication from autoregressive processes with a vector of error terms, $\boldsymbol{\varepsilon}_t = (\varepsilon_{0t}, \varepsilon_{1t}, \varepsilon_{2t}, \varepsilon_{3t}) \in \mathbb{R}^4$. This data-generating process resembles the procedures outlined in Cao and Dowd (2019) and Li (2020).

Web Figure 3 presents the width of the 95% credible (or confidence) intervals and the root-mean-square error (RMSE) for the proposed priors compared to alternative methods, across a range of κ_d values and varying percentages of spillover-affected donor units. Across all κ_d values, interval length and RMSE increase as the proportion of affected units grows, with a more significant increase for the GSC method. For both the DHS and DS2 priors, interval width and RMSE remain relatively stable across κ_d values, suggesting limited variation in estimate precision. Although, the RMSE shows some sensitivity to increased bias at higher κ_d values, particularly at $\kappa_d = 1.0$. While the BSTS model produces interval widths similar to those of the proposed priors, its coverage probability for the 95% credible intervals is below nominal (see main text), likely due to its biased estimates.

Web Appendix C.1 *Impact of distance-dependent covariate distributions*

We conduct additional experiments to assess the effect of penalizing covariate dissimilarity when baseline covariates \mathbf{X}_i are generated using distance-dependent distributions. These experiments follow the same data-generating process as in the previous section, with a modification to the generation of \mathbf{X}_i . Specifically, we redefine each covariate with a location shift: $\mathbf{X}_i = s_i \boldsymbol{\mu}_d + \tilde{\mathbf{X}}_i$, where $\tilde{\mathbf{X}}_i \stackrel{iid}{\sim} \text{MVN}(0_2, I_2)$, for $i \in [n]$. Here, $s_i \sim \text{Bernoulli}(p_i^*)$ determines if the covariate is shifted, with $p_i^* = d_i^P / \max_{j \in [n]}(d_j^P)$ based on the spatial distance d_i^P . Since $d_1^P \equiv 0$ for the treated unit, we have that $p_1^* \equiv 0$ and $\mathbf{X}_1 \equiv \tilde{\mathbf{X}}_1$. This probabilistic shift adds variability, ensuring that controls closer to the treated unit (where $p_i^* \rightarrow 0$) are more likely to remain unshifted, such that $\mathbf{X}_i \equiv \tilde{\mathbf{X}}_i$. In contrast, controls farther away (where $p_i^* \rightarrow 1$) are more likely to be shifted, giving $\mathbf{X}_i = \boldsymbol{\mu}_d + \tilde{\mathbf{X}}_i$. The location shift parameter $\boldsymbol{\mu}_d = (\mu_{1d}, \mu_{2d}) \in \mathbb{R}^2$ is pre-specified and varies across settings. We simulate 1,000 independent replications and report the results similarly to the main simulations. The location shift spans multiple scenarios with $\mu_{jd} \in \{0, 1, 5, 10\}$ for all $j = 1, 2$, where $\boldsymbol{\mu}_d = (0, 0)$ corresponds to the original setup in the main text.

Web Figures 4 and 5 presents the relative bias and coverage probability of the 95% credible (or confidence) intervals for our proposed priors compared to alternative methods across various values of κ_d and $\boldsymbol{\mu}_d$, along with different levels of spillover. In the absence of spillover, the DHS and DS2 priors demonstrate similar performance in terms of relative bias and coverage probability across all κ_d and $\boldsymbol{\mu}_d$ values, where higher values of $\boldsymbol{\mu}_d$ (i.e., $\boldsymbol{\mu}_d = 2.5, 5.0$) indicate greater covariate differences between neighboring and non-neighboring control units. There is no significant difference between using $\kappa_d = 0$

and $\kappa_d = 1$. However, with $\kappa_d = 0$, the priors tend to select non-neighboring controls, which may increase bias by including dissimilar units located farther from the treated unit. In contrast, with $\kappa_d = 1$, the priors prioritize neighboring controls, potentially reducing bias by choosing units that are more similar and spatially closer to the treated unit. Larger differences could be observed under no spillover by exploring greater magnitudes for the covariate effects; in this experiment, $\boldsymbol{\vartheta}_t = (-0.5, 0.5)$. Overall, these results indicate that spillover bias poses a more significant challenge than the estimation bias arising from selecting dissimilar control units. This is evident as performance declines with increasing κ_d , $\boldsymbol{\mu}_d$, and spillover levels, with both the DHS and DS2 priors performing similarly or worse than alternative methods when $\kappa_d = 1$. Ultimately, the improvement in relative bias and coverage probability from penalizing covariate dissimilarity is minimal, particularly when the percentage of spillover is high.

Web Appendix D. Additional Application Results

Web Figure 6 presents the time series of relative volume sales for all considered units, both at the individual and aggregate levels. Units are grouped based on whether they border Philadelphia or are the treated unit itself. Overall, Philadelphia shows a decrease in relative volume sales following the implementation of the beverage tax on January 1, 2017. In contrast, average sales for ZIP3 areas bordering Philadelphia increase post-tax, while ZIP3 areas not bordering Philadelphia maintain regular sales, reflecting stationarity.

Web Figure 7 presents two maps of the ZIP3 areas: one showing the change in average relative volume sales before and after the beverage tax, and the other depicting covariate similarity between control units and Philadelphia (the treated unit). On average, volume sales in Philadelphia decline following the tax implementation (dark blue in the left panel), while neighboring areas show an increase. Other regions exhibit minimal change in beverage sales. Covariate similarity, measured by the weighted distance $d_{i,1}^C$ with $\kappa_d = 1$, indicates that most control units are not very similar to Philadelphia, except for Baltimore (dark orange in the right panel), which shows a higher similarity to Philadelphia.

Web Figure 8 presents trace plots for τ_t at four randomly selected post-intervention times $t > T_0$, with a single chain randomly selected for the DHS and DS2 priors using $\kappa_d = 0$. The trace plots display the post-warmup period over 5,000 iterations, indicating good mixing and convergence for the Markov chains, which suggests an efficient exploration of the posterior distribution.

Web Figure 9 presents the estimated causal effect of the beverage tax using the DS2 prior across various

cutoff ρ values, each representing geographic boundaries as $\kappa = 0$. Each cutoff excludes increasingly larger percentages of control units from the donor pool, ranging from 0% to 50% in 5% increments. The pre-intervention fit is omitted to highlight post-intervention estimation differences. Results show a significant reduction in sugar-sweetened and artificially sweetened beverage sales at mass merchandise stores in Philadelphia, with all four-week 95% credible intervals indicating a non-zero and negative policy effect (i.e., $\tau_t < 0$). Despite an increase in average sales for ZIP3 areas bordering Philadelphia (Web Figure 6), no clear positive spillover effect is observed, as the estimated reduction of sales increases as more neighboring controls are excluded. This pattern may result from the DS2 prior not selecting bordering areas affected by spillover, as other areas may contribute more to the model's predictive power. Overall, this suggests that spillover has a minimal impact on estimating the effect of the beverage tax.

Category	Notation	Support	Definition
Data	Y_{1t}	$Y_{1t} \in \mathbb{R}$	The outcome for the treated unit at time t .
	$\mathbf{Z}_t = (\mathbf{Z}_{1t}, \dots, \mathbf{Z}_{nt})$	$\mathbf{Z}_{it} \in \{0, 1\}$	The binary treatment assignments for all units at time t .
	$\mathbf{V}_t = (Y_{2t}, \dots, Y_{nt})$	$Y_{it} \in \mathbb{R}$	The outcomes for the control units in the donor pool at time t .
	$d_{i,1}^C$	$d_{i,1}^C \in [0, 1]$	The weighted distance between the treated unit and control i .
Parameters	$\boldsymbol{\beta} = (\beta_2, \dots, \beta_n)$	$\beta_i \in \mathbb{R}$	The synthetic control coefficients.
	φ	$\varphi \in \mathbb{R}$	The effect of the previously observed outcome for the treated unit.
	ϕ	$\phi \in \mathbb{R}^+$	The time-invariant variance for the treated unit outcomes.
	$\mu_\varphi, \sigma_\varphi$	$\mu_\varphi \in \mathbb{R}, \sigma_\varphi \in \mathbb{R}^+$	The hyperparameters for φ .
	ν_ϕ, τ_ϕ	$\nu_\phi \in \mathbb{R}^+, \tau_\phi \in \mathbb{R}^+$	The hyperparameters for ϕ .
DHS	$\boldsymbol{\lambda} = (\lambda_2, \dots, \lambda_n)$	$\lambda_i \in \mathbb{R}^+$	The local shrinkage parameter for β_i .
	ζ	$\zeta \in \mathbb{R}^+$	The global shrinkage parameter for all β_i 's.
DS2	$\boldsymbol{\omega} = (\omega_2, \dots, \omega_n)$	$\omega_i \in \{0, 1\}$	The component assignment for β_i .
	ν	$\nu \in \mathbb{R}^+$	The variance parameter for the normally distributed slab component.
Others	ρ	$\rho \in [0, 1]$	The cutoff for distance-dependent assignment mechanism.
	κ_d	$\kappa_d \in [0, 1]$	The importance weight for the weighted distance function $d_C(\cdot)$.
	$\delta_0(u)$		The Dirac delta function centered at zero.
	$\mathbb{1}(\cdot)$		The indicator function.
	$\mathbf{0}_n = (0, \dots, 0)$		The n -length zero vector.

Abbreviations: Distance-based horseshoe (DHS) prior; distance-based spike-and-slab (DS2) prior.

Web Table 1: Key notations of the distance-based priors described in the main text.

Data-Generating Process

$$\delta_t = 1 + 0.5\delta_{t-1} + \varepsilon_{0t}$$

$$\boldsymbol{\vartheta} = (-0.5, 0.5)$$

$$f_{1t} = 0.5f_{1(t-1)} + \varepsilon_{1t}$$

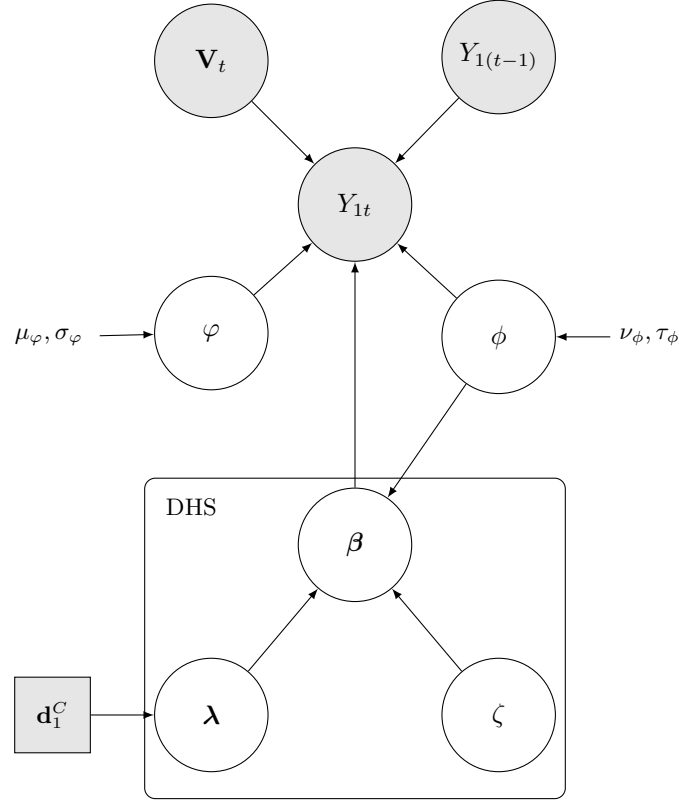
$$f_{2t} = 1 + 0.5f_{2(t-1)} + \varepsilon_{2t}$$

$$f_{3t} = 0.5f_{3(t-1)} + \varepsilon_{3t}$$

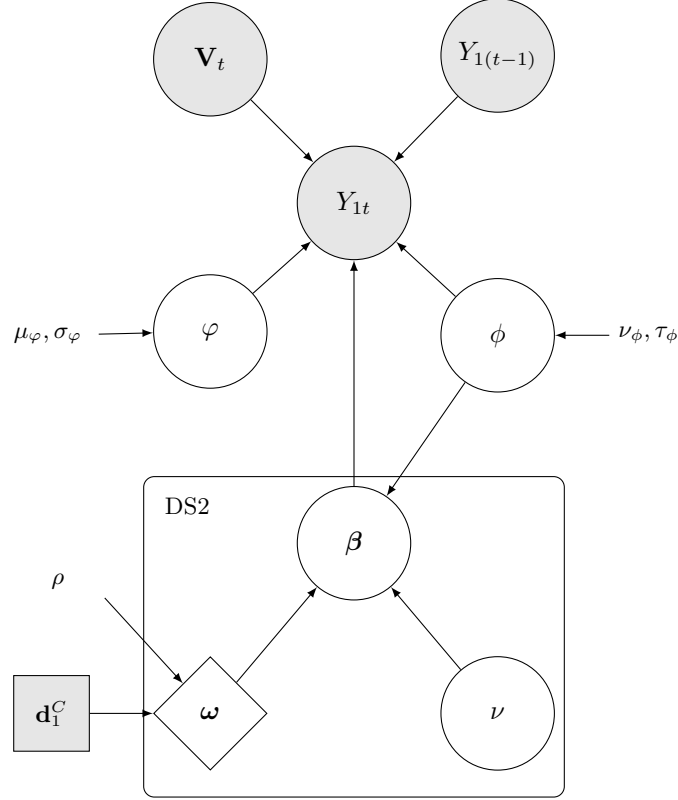
$$\mu_{ik} \stackrel{iid}{\sim} \text{Uniform}(0, 1), \quad \text{for } k = 1, 2, 3$$

$$\boldsymbol{\varepsilon}_t \stackrel{iid}{\sim} \text{MVN}(0_4, I_4)$$

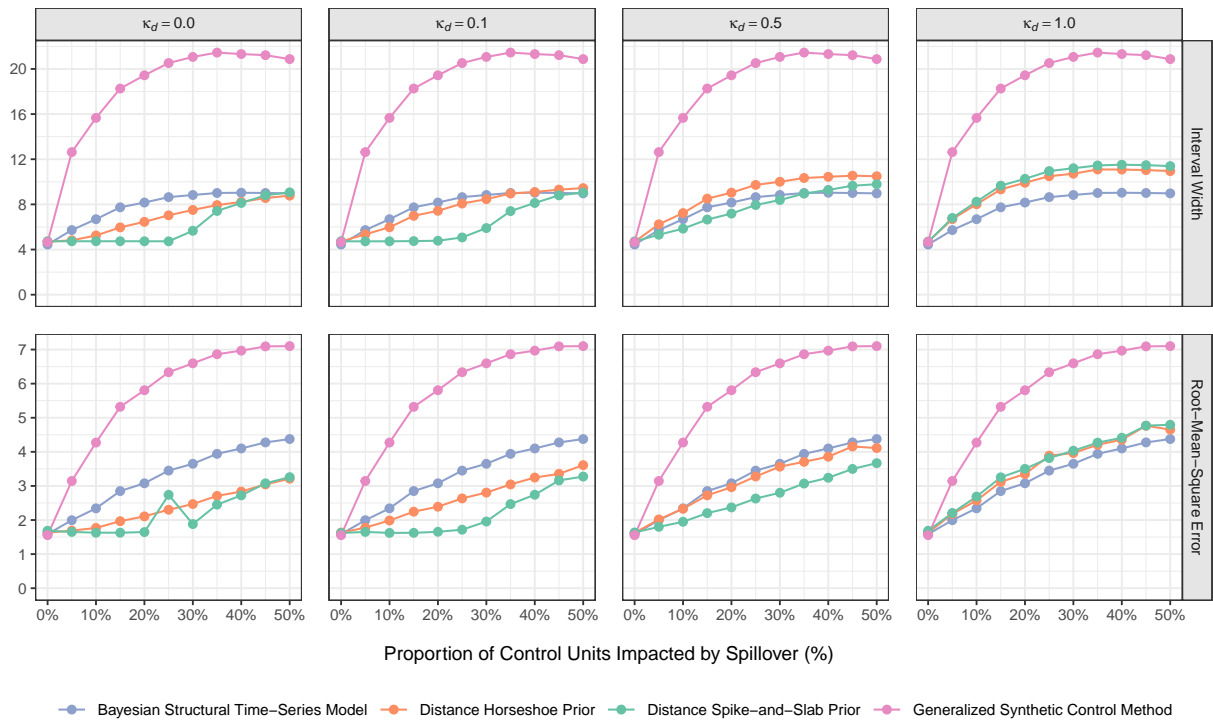
Web Table 2: Data-generating process for parameters in the linear three-factor model used in simulations.



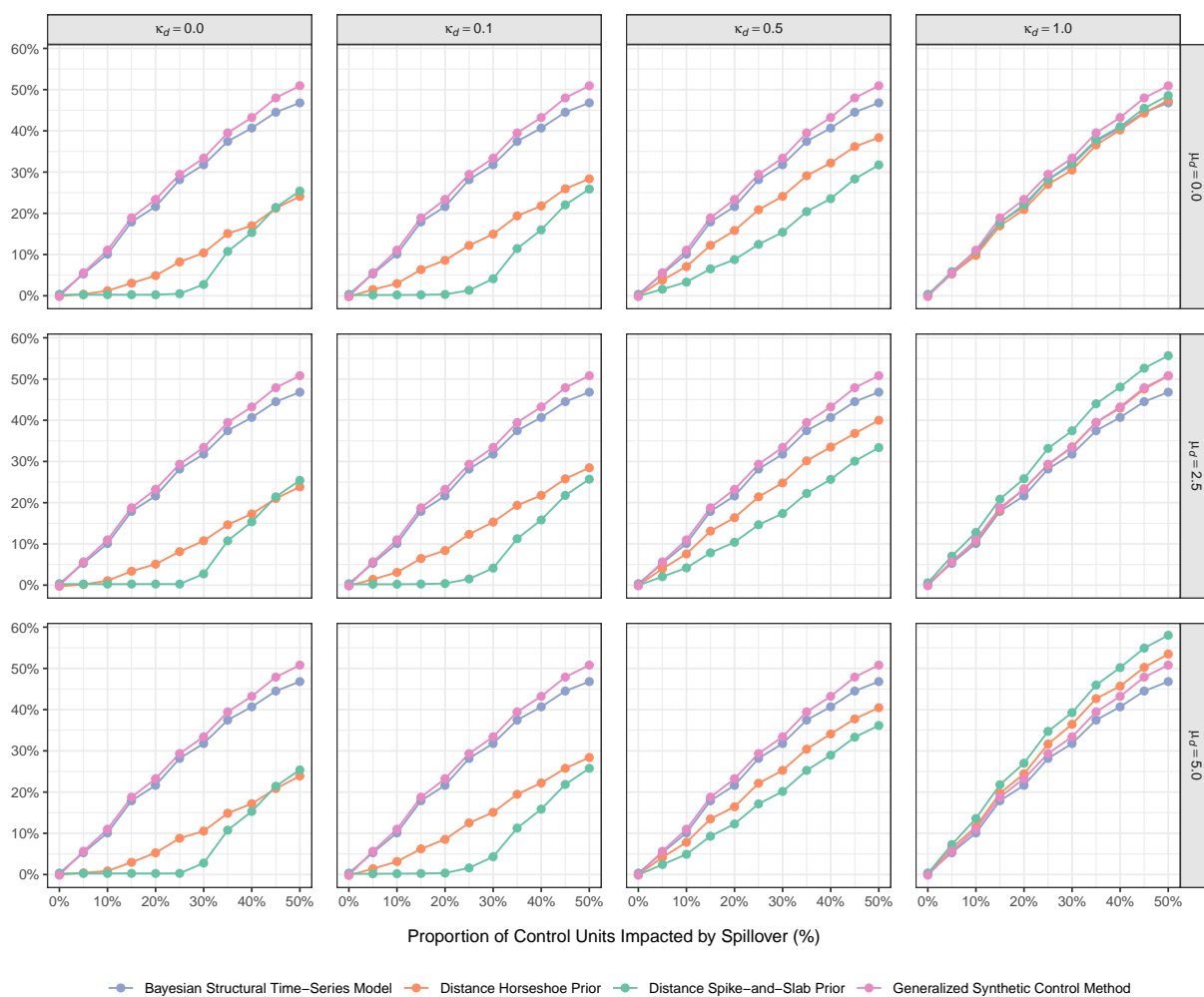
Web Figure 1: Graphical representation of the outcome model with the distance-based horseshoe (DHS) prior. Observed pre-intervention outcomes, Y_{1t} , are modeled as a function of outcomes in the donor pool, \mathbf{V}_t , and the previous outcome, $Y_{1(t-1)}$. The covariate effect of the previous outcome, φ , follows a Normal prior with hyperparameters μ_φ and σ_φ . Outcome variance, ϕ , follows a half-Student's t prior with hyperparameters ν_ϕ and τ_ϕ . SC coefficients, β , follow the DHS prior with hyperparameters λ and ζ , where $\lambda = (\lambda_2, \dots, \lambda_n)$ incorporates an empirical hyperprior based on weighted distances, $\mathbf{d}_1^C = (d_{2,1}^C, \dots, d_{n,1}^C)$. Gray-filled circles indicate observations, while constant hyperparameters are unshaped; data for the empirical prior is represented by a square. Parameters comprising the DHS prior are outlined.



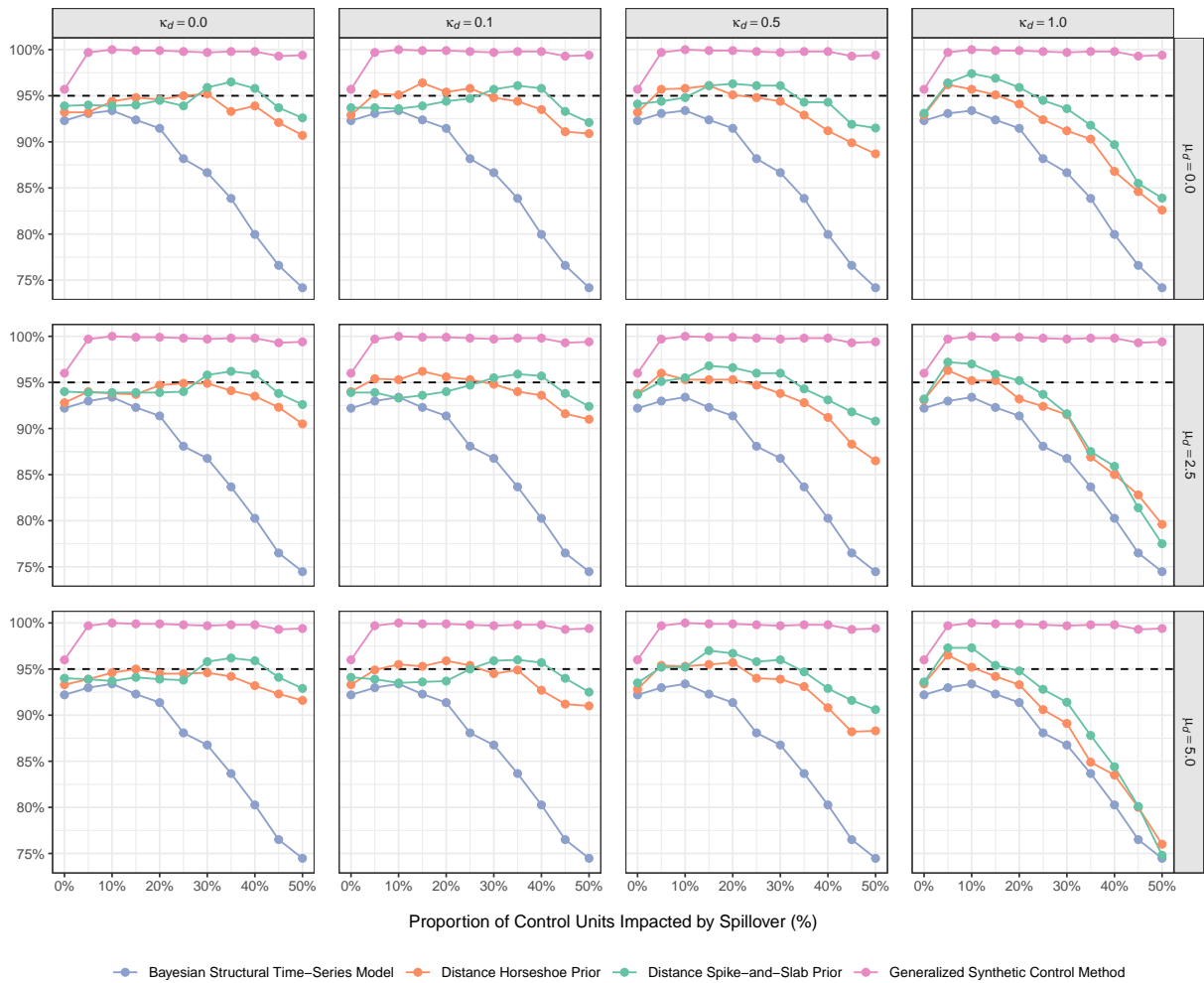
Web Figure 2: Graphical representation of the outcome model with the distance-based spike-and-slab (DS2) prior. Observed pre-intervention outcomes, Y_{1t} , are modeled as a function of outcomes in the donor pool, \mathbf{V}_t , and the previous outcome, $Y_{1(t-1)}$. The covariate effect of the previous outcome, φ , follows a Normal prior with hyperparameters μ_φ and σ_φ , while the outcome variance, ϕ , follows a half-Student's t prior with hyperparameters ν_ϕ and τ_ϕ . SC coefficients, β , follow the DS2 prior with hyperparameters ω and ν , where $\omega = (\omega_2, \dots, \omega_n)$ are deterministic indicator functions based on a user-specified parameter, ρ , and weighted distances, $\mathbf{d}_1^C = (d_{2,1}^C, \dots, d_{n,1}^C)$. Gray-filled circles indicate observations, constant hyperparameters are unshaped, the deterministic parameter is shown by a diamond, and data for the empirical prior is represented by a gray-filled square. Parameters comprising the DS2 prior are outlined.



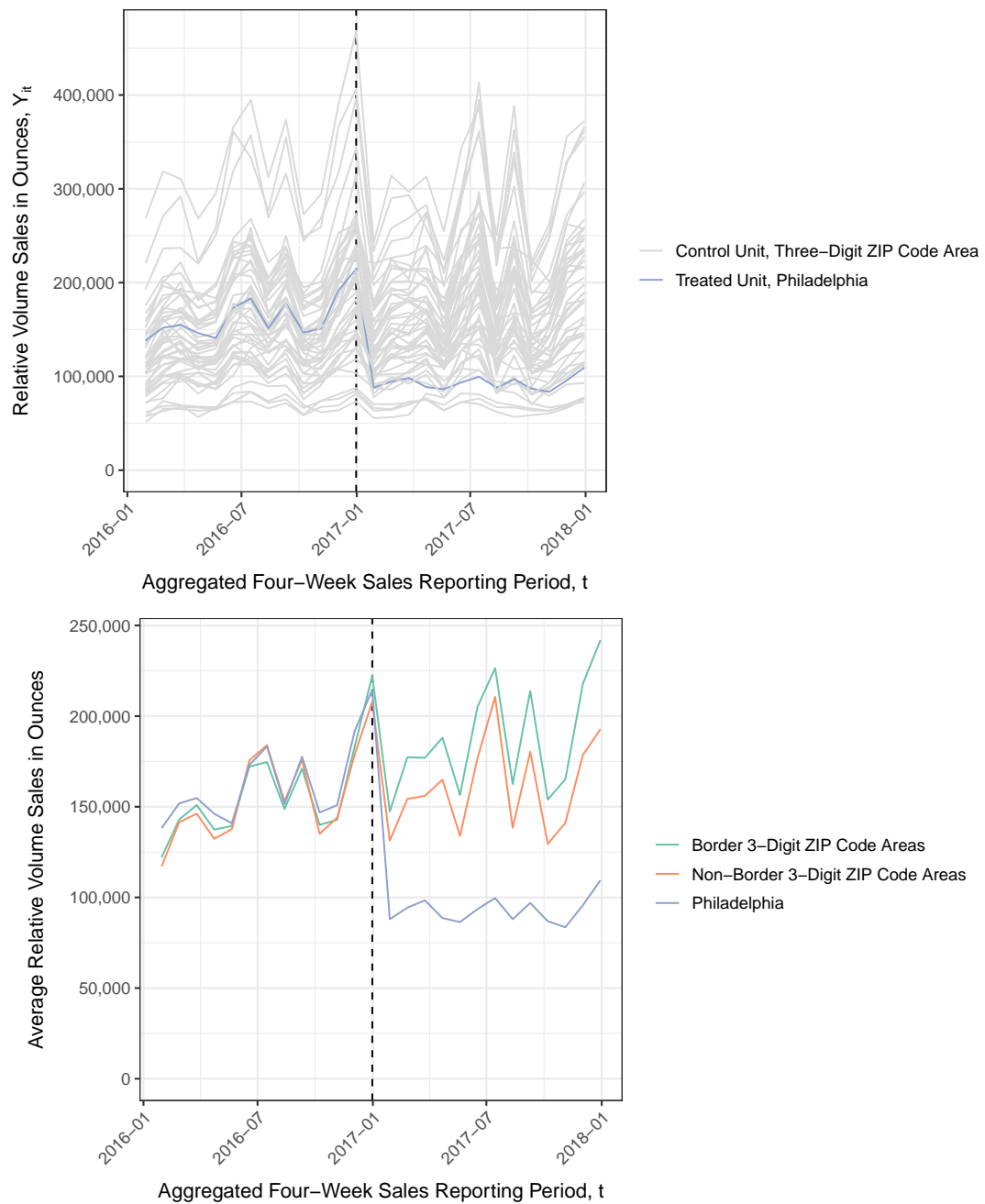
Web Figure 3: Finite-sample interval width (upper panels) and root-mean-square error (lower panels) across 1,000 replicates with $T_0 = 30$ pre-intervention periods and $J = 50$ control units, comparing our distance-based priors to alternative methods. Results are shown for varying values of κ_d and spillover magnitudes. Interval width is based on 95% credible (or confidence) intervals, while root-mean-square error is calculated as the square root of the variance plus the squared bias.



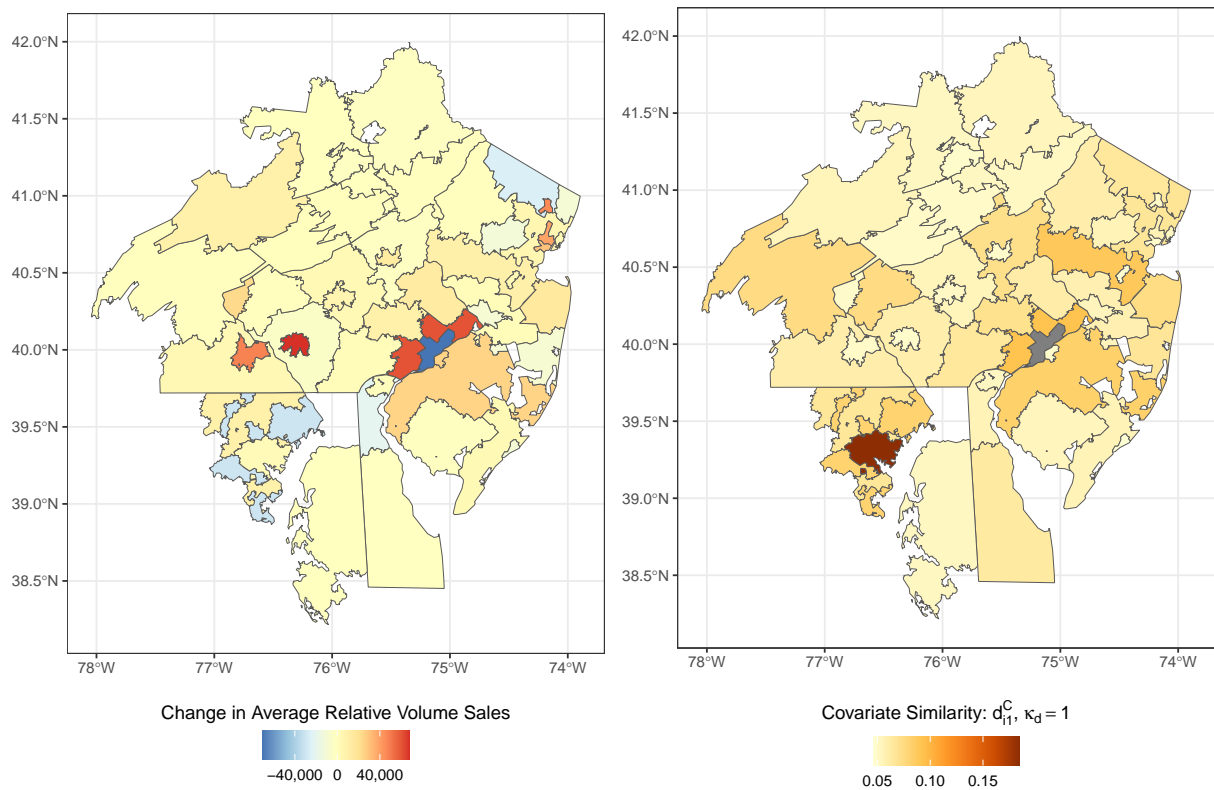
Web Figure 4: Finite-sample relative bias across 1,000 replicates with $T_0 = 30$ pre-intervention periods and $J = 50$ control units, comparing our distance-based priors to alternative methods. Results are shown for varying values of κ_d , μ_d , and spillover magnitudes. Bias is relative to the true effect ($\tau_t = 7$).



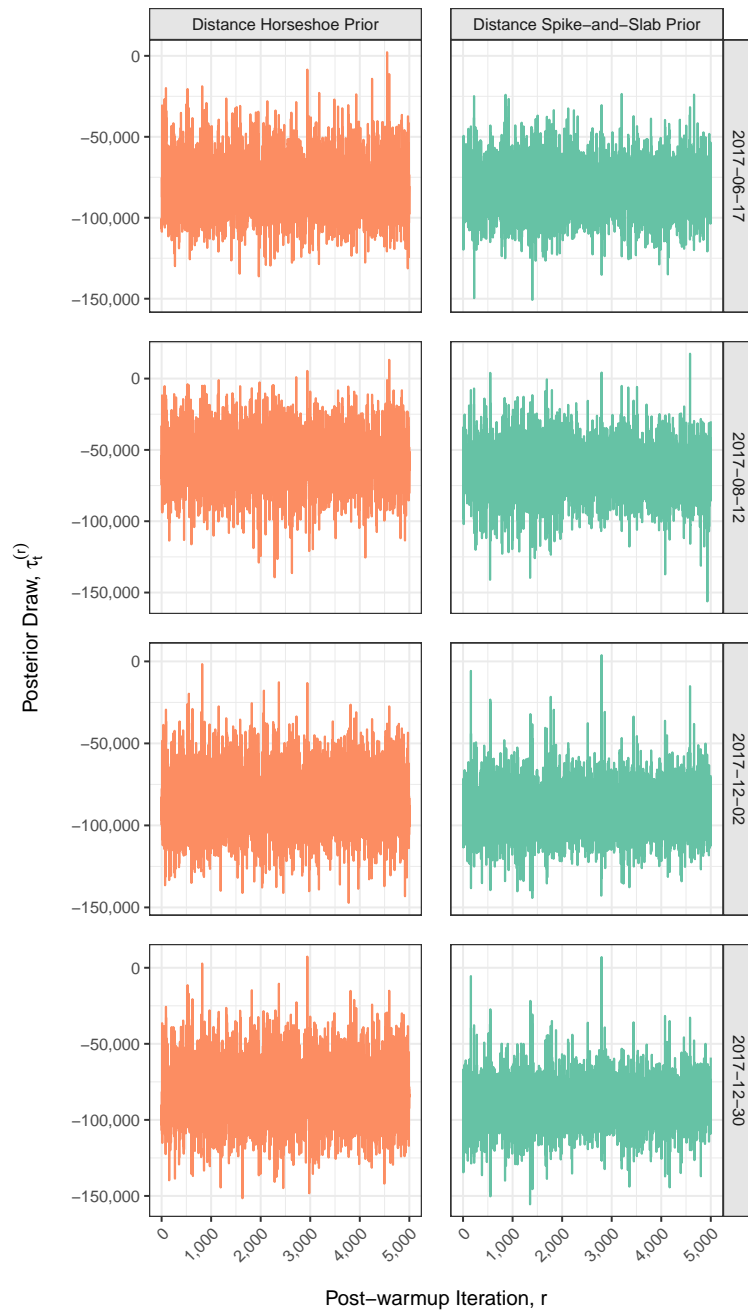
Web Figure 5: Finite-sample coverage probability across 1,000 replicates with $T_0 = 30$ pre-intervention periods and $J = 50$ control units, comparing our distance-based priors to alternative methods. Results are shown for varying values of κ_d , μ_d , and spillover magnitudes. Coverage probability is based on 95% credible (or confidence) intervals. The dashed horizontal line represents the 95% nominal coverage level.



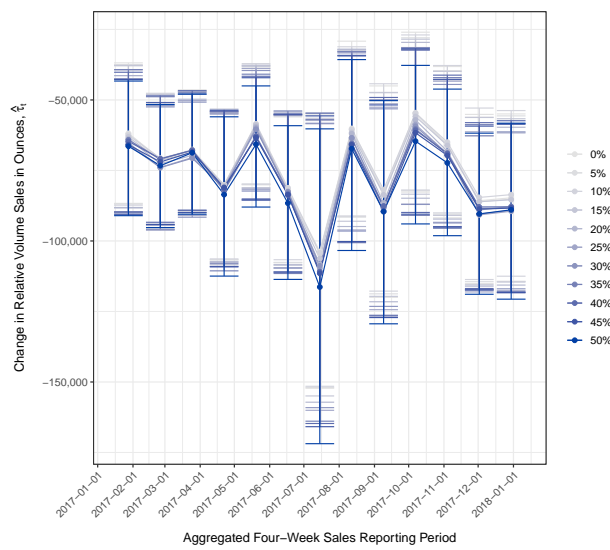
Web Figure 6: Time-series plots of relative volume sales, shown at the unit level (top panel) and aggregated (bottom panel). Volume sales are measured in ounces, adjusted by the number of stores in each ZIP3 area. Unit-level time series are grouped by treatment status at the intervention date. The aggregated series represent total sales for Philadelphia and average sales across ZIP3 areas that either border or do not border Philadelphia.



Web Figure 7: Map of ZIP3 areas showing the change in average relative volume sales (top panel) and covariate similarity between each control unit and the treated unit (right panel). The change in volume sales was calculated as the difference in average sales before and after the tax implementation. Covariate similarity is represented by the weighted distance $d_{i,1}^C$ with $\kappa_d = 1$.



Web Figure 8: Trace plots for τ_t at four randomly selected post-intervention times ($t > T_0$) and for a single randomly chosen chain (from 1 to 4) under the DHS and DS2 priors with $\kappa_d = 0$. Each panel shows the post-warmup period, with the initial 5,000 iterations are discarded as burn-in, and the subsequent 5,000 iterations are used for inference.



Web Figure 9: Posterior mean and 95% credible interval pointwise estimates for the causal effect τ_t of the beverage tax on relative volume sales in Philadelphia, shown across different assumptions on the percentage of control units affected by spillover for the DS2. The cutoff ρ is set according to the sample quantiles of the weighted distances, given the percentage, and using $\kappa_d = 0$. Estimates are calculated for each post-intervention four-week aggregated period $t > T_0$.